



Bitlis Eren University Journal of Science and Technology

Year: 2024 • Volume: 14 • Issue: 2

ISSN: 2146-7706

Contact:

BEU Journal of Science and Technology, Bitlis Eren Üniversitesi 13000, Merkez, Bitlis/ TÜRKİYE
Tel: 0 (434) 222 0000

beujstd@beu.edu.tr <https://dergipark.org.tr/tr/pub/beuscitech>



Bitlis Eren University Journal of Science and Technology

e-ISSN	:	2146-7706
Date of Issue	:	December 26, 2024
Issue Period	:	December 2024
Volume	:	14
Issue	:	2
Founded	:	2011
Location	:	Bitlis
Language	:	English
Address	:	Bitlis Eren University Journal of Science and Technology Bitlis Eren Üniversitesi 13000, Merkez, Bitlis/ TÜRKİYE
e-mail	:	beujstd@beu.edu.tr
URL	:	https://dergipark.org.tr/tr/pub/beuscitech

Bitlis Eren University Journal of Science and Technology

Year: 2024 • Volume: 14 • Issue: 2

Editorial Board

On behalf of Bitlis Eren University **Prof. Dr. Necmettin ELMASTAŞ**
Owner *Bitlis Eren University*

Editor-in-Chief **Assist. Prof. Dr. Ufuk KAYA**
Bitlis Eren University

Co-Editor **Assist. Prof. Dr. Kerim ÖZBEYAZ**
Bitlis Eren University

Co-Editor **Assist. Prof. Dr. Ömer KARABEY**
Bitlis Eren University

Language Editor **Lecturer Ahmet ÖZKAN**
Bitlis Eren University

Editorial Board **Prof. Dr. Mehmet Cihan AYDIN**
Bitlis Eren University

Prof. Dr. Zeynep AYGÜN
Bitlis Eren University

Prof. Dr. Murat KARAKAŞ
Bitlis Eren University

Assoc. Prof. Dr. Engin YILMAZ
Bitlis Eren University

Assoc. Prof. Dr. Musa ÇIBUK
Bitlis Eren University

Assoc. Prof. Dr. Fahrettin ÖZBEY
Bitlis Eren University

Assoc. Prof. Dr. Behçet KOCAMAN
Bitlis Eren University

Assoc. Prof. Dr. Faruk ORAL
Bitlis Eren University

Assoc. Prof. Dr. Tülay ÇEVİK SALDIRAN
Bitlis Eren University

Assoc. Prof. Dr. Ramazan ERDOĞAN
Bitlis Eren University

Bitlis Eren University Journal of Science and Technology

Year: 2024 • Volume: 14 • Issue: 2

Bitlis Eren University Journal of Science and Technology (Bitlis Eren Univ J Sci & Technol) is an international, refereed open access electronic journal. Research results, reviews and short communications in the fields of Agriculture, Biology, Chemistry, Engineering Sciences, Mathematics, Medicinal, Molecular and Genetics, Physics, Statistics, and also Engineering Sciences are accepted for review and research article publications. Papers will be published in English. Scientific quality and scientific significance are the primary criteria for publication. Articles with a suitable balance of practice and theory are preferred. Manuscripts previously published in other journals and as book sections will not be accepted.


Bitlis Eren University Journal of Science and Technology indexed in:

- EBSCO
- SCILIT
- ACARINDEX
- SOBIAD
- ACADEMINDEX

Bitlis Eren University Journal of Science and Technology

Year: 2024 • Volume: 14 • Issue: 2

Articles

İlker Kara 

TWIN GHOSTS: EVIL TWIN ATTACKS IN WIRELESS NETWORKS AND DEFENSE MECHANISMS 58-74

Larry Orobome Agberegha , Joseph Oyekale 

EXERGO-ENVIRONMENTAL SUSTAINABILITY ASSESSMENTS OF ORGANIC RANKINE CYCLE PLANTS POWERED BY A TYPICAL ABANDONED OIL WELL 75-102

Sultan Şahin Bal , Yonca Dervişoğlu Koç 

DETERMINATION OF RADON GAS LEVELS IN THE AIR IN THE FACULTY BUILDING (BİTLİS) 103-118

2007



TWIN GHOSTS: EVIL TWIN ATTACKS IN WIRELESS NETWORKS AND DEFENSE MECHANISMS

İlker Kara¹ 

¹ Çankiri Karatekin University, Department of Computer Engineering, Çankırı, Türkiye,
karaikab@gmail.com

KEYWORDS

Evil twin attack
Security
Wireless access point
Fake access point

ARTICLE INFO

Research Article

DOI

[10.17678/beuscitech.1450756](https://doi.org/10.17678/beuscitech.1450756)

Received 11 March 2024

Accepted 25 December 2024

Year 2024

Volume 14

Issue 2

Pages 58-74



ABSTRACT

With the increasing adoption of wireless network technologies, a variety of attacks targeting these networks have emerged, posing significant threats to user security. One prominent type of attack is the evil twin attack, which involves the creation of fake access points, often referred to as "evil twins." In this type of attack, a malicious actor sets up a fake access point (AP) designed to closely resemble a legitimate one, thereby deceiving users into believing it is trustworthy. By exploiting these fake APs, attackers can capture user credentials and gain unauthorized access to sensitive information, potentially leading to financial exploitation or system breaches. Due to the covert nature of evil twin attacks, they can be highly effective without the users' awareness. In this study, explores the risks posed by evil twin attacks and investigates defense strategies to address the security challenges in wireless networks. To achieve this, a scenario involving an evil twin attack is developed and analyzed. In this scenario, an attacker establishes a fake wireless access point in a café or public area near the targeted institution, replicating the institution's network name and security settings to trick users into connecting to the malicious network. This study underscores the potential impacts of such attacks and outlines critical measures that both users and institutions should implement to safeguard against these threats.

1 INTRODUCTION

The widespread adoption of wireless network technologies in today's world has led to a significant transformation in the field of information and communication [1]. However, along with the proliferation of this technology, malicious attackers have developed various types of attacks targeting wireless networks, posing threats to the security of users. One of the most sophisticated types of these attacks is a form of attack known as the evil twin attack. The evil twin attack is executed through the creation of fake access points [2]. These attacks typically involve the creation of a fake access point that mimics the appearance of a wireless access point that users perceive as trustworthy. As soon as the victim connects to this fake access point, the attack is initiated. Evil twin attacks enable attackers to steal the identities and passwords of legitimate users and gain access to sensitive data using this information [3]. This poses a serious threat to both the security of users and the information security of institutions.

In recent years, the most common analysis methods used for preventing and detecting evil twin attacks involve monitoring and analyzing network traffic, analyzing security protocols, and utilizing artificial intelligence and machine learning techniques [4]. The method based on monitoring and analyzing network traffic relies on analyzing situations where the number and types of packets in the network traffic are different from normal, enabling the detection of a potential evil twin attack. Another method used to prevent evil twin attacks is the use of security protocols. In particular, strong encryption and authentication methods can prevent malicious actors from creating fake access points. By ensuring that users securely connect to the network, this method can reduce the impact of evil twin attacks [4]. Another approach used for detecting and preventing evil twin attacks involves the use of artificial intelligence and machine learning techniques. These methods are used to analyze large datasets to detect abnormalities and signs of attacks. In particular, deep learning algorithms have the potential to identify and block complex evil twin attacks [5].

This study aims to address security threats in wireless networks and specifically examine the potential risks of and protection strategies against evil twin attacks. The overall objective of the study is twofold. Firstly, a case analysis was

conducted to understand how evil twin attacks are carried out. The goal here is to provide concrete recommendations to elucidate the logic behind the attacker's evil twin attack. Secondly, the study aims to explain the complexity of evil twin attacks and their impact on cybersecurity, as well as to develop mechanisms for protection against these attacks. In this study, differentiates itself from existing tools used for modeling evil twin attacks by proposing a novel prevention mechanism that incorporates advanced security protocols and user education. While most existing literature focuses primarily on the process of executing the attack, this paper provides an in-depth analysis of both the technical aspects of the attack and the effective countermeasures that can be employed to mitigate such threats.

Within this scope, an evil twin attack scenario was created and analyzed. In this scenario, the attacker sets up a fake wireless access point in a cafe or public area near the targeted institution, designing the fake access point to mimic the name and security settings of the target institution to lure users into connecting to the fake network under their control. This study not only highlights the potential impacts of evil twin attacks but also includes significant steps in understanding the strategies of attackers and taking necessary measures to protect users and institutions against such attacks through complementary mechanisms.

2 MATERIAL AND METHOD

This section begins by providing a detailed explanation of the equipment and steps used to carry out the evil twin attack (real case study). Subsequently, a brief description of the events occurring during the attack is provided.

2.1 Equipment

The equipment used to carry out the evil twin attack consists of several basic components. These are:

1. Kali Linux Operating System: A powerful pentesting operating system like Kali Linux is necessary for the successful execution of the attack. Kali Linux is a Debian-based operating system that includes numerous cybersecurity tools and applications.

2. **Computer:** A suitable computer and monitor are required to execute the evil twin attack. This computer should be compatible with the Kali Linux operating system and will be used to manage the attack. In this study, a Lenovo workstation with an Intel Core i7-10700K processor, 32GB RAM, 1TB HDD, 512GB SSD, and a 5GB Quadro GPU running Windows 11 Pro operating system was used.
3. **Network Interface Card (NIC):** An NIC capable of conducting network discovery and supporting monitor mode is essential for effectively executing the attack. In this scenario, an Alfa Network NIC was used because it supports monitor mode and has the capability to monitor network traffic.

2.2 Attack Steps

This section focuses on the attack steps of evil twin attacks in wireless networks. These steps will explain how attackers create fake networks and acquire user credentials (Figure 1). The attack steps are as follows [6]:

1. **Installation of Kali Linux Operating System:** As the first step, the attacker installs the Kali Linux operating system on a suitable computer. Kali Linux comes pre-loaded with many cybersecurity tools and provides an ideal environment for pentesting operations.
2. **Network Card Settings:** The attacker enables monitor mode using the Alfa Network network card and makes it available to monitor network traffic. This step is crucial for discovering devices on the network and determining targets.
3. **Initiation of Evil Twin Attack:** The attacker initiates the evil twin attack to steal the identities of legitimate users on the target network. This involves generating fake requests or transactions and manipulating network traffic. The attacker creates fake network requests and redirects network traffic to deceive target devices. To achieve this, the attacker runs the Aircrack-ng tool on Kali Linux to detect security vulnerabilities in wireless networks. This step is important for analyzing target networks and identifying potential targets.
4. **Unauthorized Access:** When the evil twin attack is successfully executed, the attacker captures the identities of legitimate users and gains unauthorized

access to systems. This aims to gain access to sensitive data, take control of systems, or perform other malicious activities. For this purpose, the Aircrack-ng tool is used to generate fake requests or transactions and manipulate network traffic.

5. Monitoring and Improvement: The attacker monitors and improves the effectiveness of the attack. By analyzing network traffic, they identify discovered vulnerabilities and develop strategies for future attacks.

These steps provide a general approach to executing an evil twin attack. However, each attack situation is unique and may vary depending on the attacker's goals and environmental factors [7], [8].

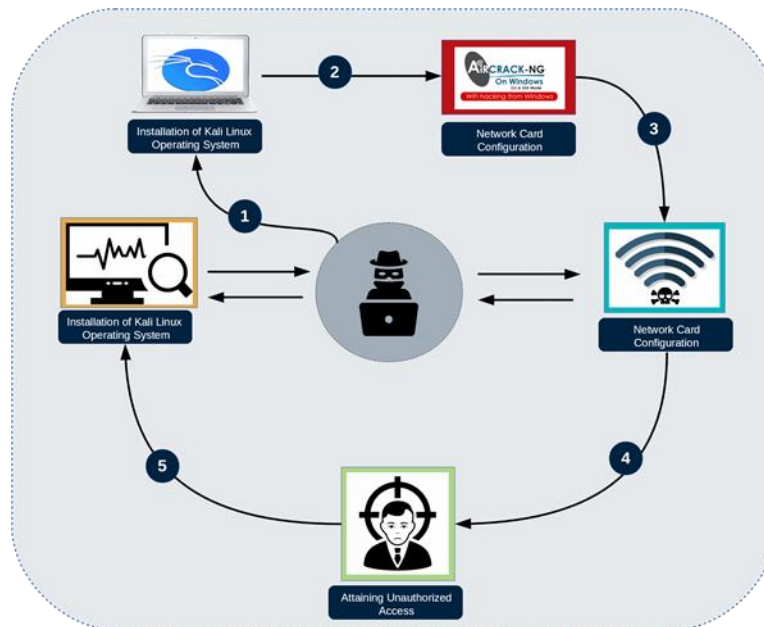


Figure 1. Evil Twin attack steps [9].

2.3 Evil Twin Attack Scenario

The steps of the evil twin attack are provided in Figure 1. The attack begins with the attacker installing the Kali Linux operating system on a suitable computer. Then, the attacker runs the Aircrack-ng tool on Kali Linux to detect security vulnerabilities in wireless networks. This step is crucial for analyzing target networks and identifying potential targets. Subsequently, the attacker initiates the evil twin attack to steal the identities of legitimate users on the target network. By using the Aircrack-ng tool, fake requests or transactions are generated, and network traffic is manipulated [10]. When the evil twin attack is successfully executed, the attacker

captures the identities of legitimate users and gains unauthorized access to systems. This step aims to gain access to sensitive data, take control of systems, or perform other malicious activities. Finally, the attacker monitors and improves the effectiveness of the attack. By analyzing network traffic, they identify discovered vulnerabilities and develop strategies for future attacks.

3 ANALYSIS OF CASE STUDY

In this section, a case analysis was conducted to understand how evil twin attacks are carried out. For this purpose, a real-life case example was examined, and a comprehensive analysis was conducted on the methods used to execute the evil twin attack and the results obtained. Airgeddon tool package was utilized for this purpose. Airgeddon is equipped with various features that allow monitoring and controlling of wireless networks, including menu-driven handshake capturing and Evil Twin Attack functionalities.

Figure 2 shows how the necessary preparations for the malicious twin attack are made through the user interface of the Airgeddon tool. Initially, the user needs to redirect their wireless network card to the correct network and activate monitoring mode. Subsequently, by selecting the sixth option, "Evil Twin Attack (AP encryption)," preparations are made to create a fake access point. This fake access point enables the attacker to redirect users of the target network to a login page that appears legitimate, thereby capturing their credentials.

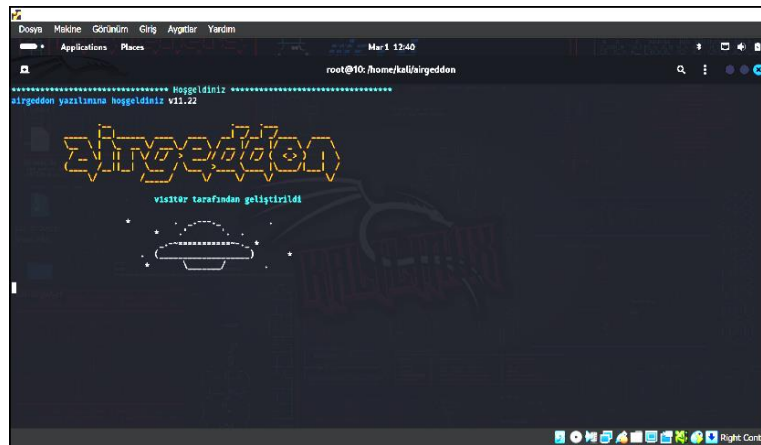


Figure 2. Airgeddon Tool installation page

Figure 2 depicts a desktop environment running the Kali Linux operating system, commonly used for education and research purposes in the field of cybersecurity. Within Kali Linux, the open-source tool Aircgeddon comes pre-installed.

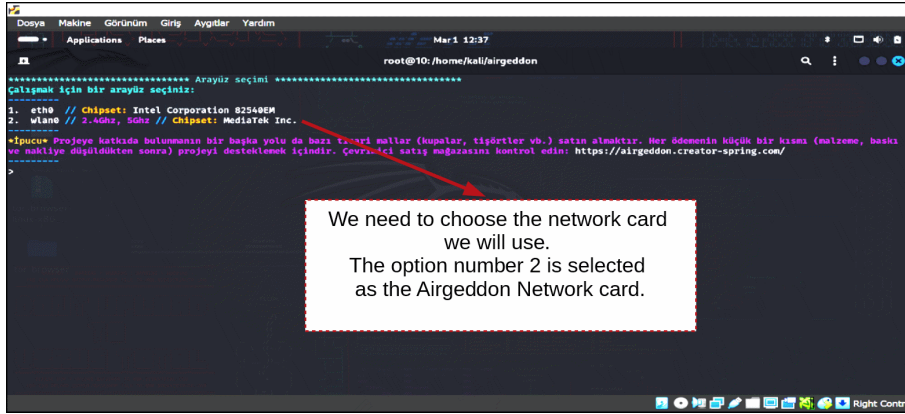


Figure 3. Configuration of Aircgeddon tool.

Figure 3 shows the step where users select their wireless network cards and then configure the necessary settings on these cards for using the Aircgeddon tool. In this step, the network card to be used in the attack is selected. Subsequently, the type of attack to be performed is chosen from the parameters available in the Aircgeddon tool menu (Figure 4).

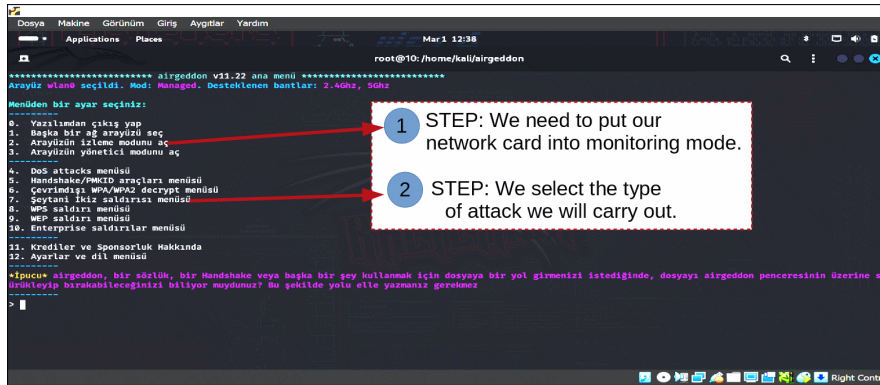


Figure 4. Configuration of Aircgeddon tool.

Figure 4 shows the user interface and usage parameters of the wireless penetration testing tool called Aircgeddon. For this purpose, the first step is to set the network card to monitoring mode. Subsequently, the type of attack to be performed should be determined. A two-step process involving setting the wireless network cards to monitoring mode and selecting the type of attack to be performed is shown. In the first step, users need to select the network card to switch to

prompted to enter their credentials, creating an illusion of connecting to the authentic network.

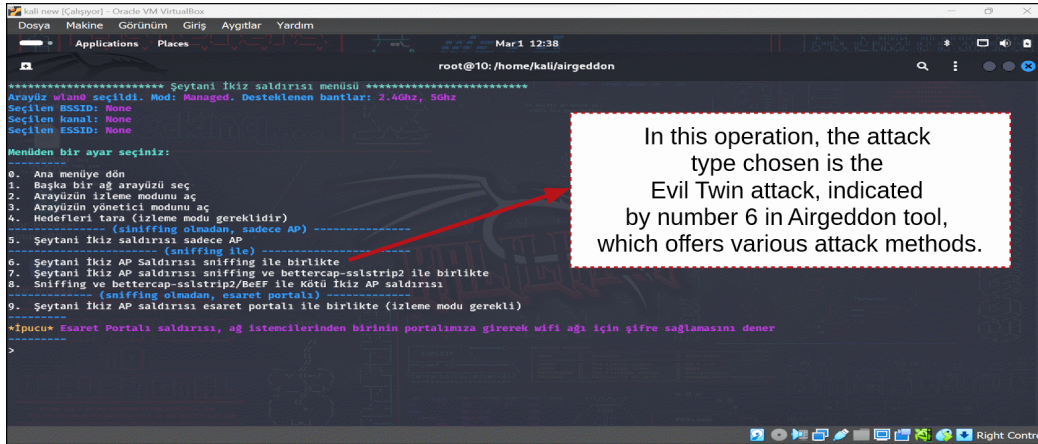


Figure 6. Selection of an Evil Twin attack type using the Airgeddon tool.

Following this step, the target network is identified, and the Evil Twin attack is initiated using the Airgeddon tool. As the attack commences, the perpetrator enters a waiting phase, displaying a series of interfaces and screens. In this attack methodology, the expected waiting time typically varies between 1 to 45 minutes (ref). During the attack, the perpetrator forcibly disconnects users from the current network through a deauthentication (death) process, compelling them to connect to the perpetrator's fake network (Figure 7). This strategy aims to deceive users into connecting to the fake network, resembling a genuine one, in order to obtain the victim's credentials.



Figure 7. Selection of an Evil Twin attack type using the Airgeddon tool.

Among the various deauthentication methods available in the Airgeddon tool, the perpetrator selects the one they consider most effective, often identified as

“Death aireplay attack” (number 2) (Figure 7). This method targets all devices on the network using the aireplay-ng tool, causing them to disconnect from the network and thus forcing users to reconnect. Once the channel hopping feature is disabled and the selected interface is confirmed, the perpetrator awaits users to connect through the fake network (Figure 7).

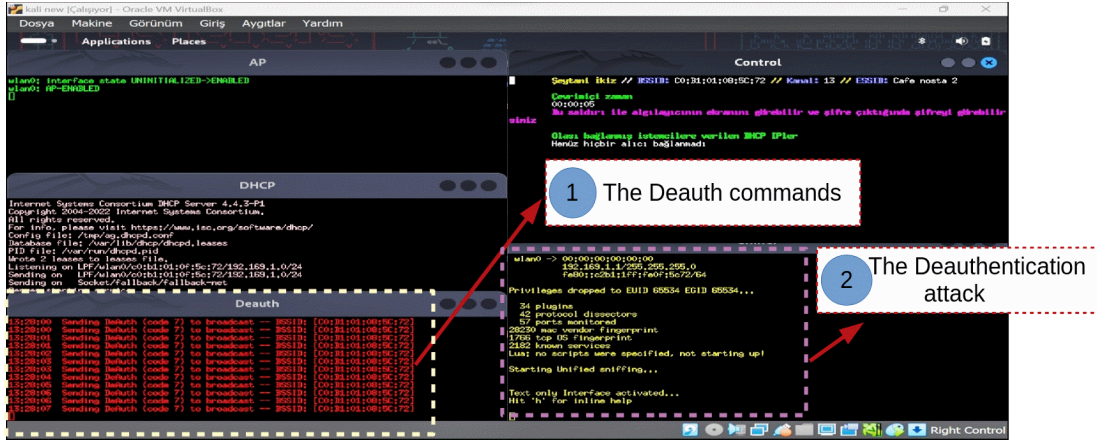


Figure 8. The Death commands and the moment of deauthentication attack.

In Figure 8 (1), continuous “Death” commands are observed. This method is used to disconnect users from the legitimate network and force them to connect to the perpetrator's fake network. The deauthentication attack disrupts users' current connections, prompting them to automatically reconnect to the strongest signal, which in this case would be the perpetrator's fake network.

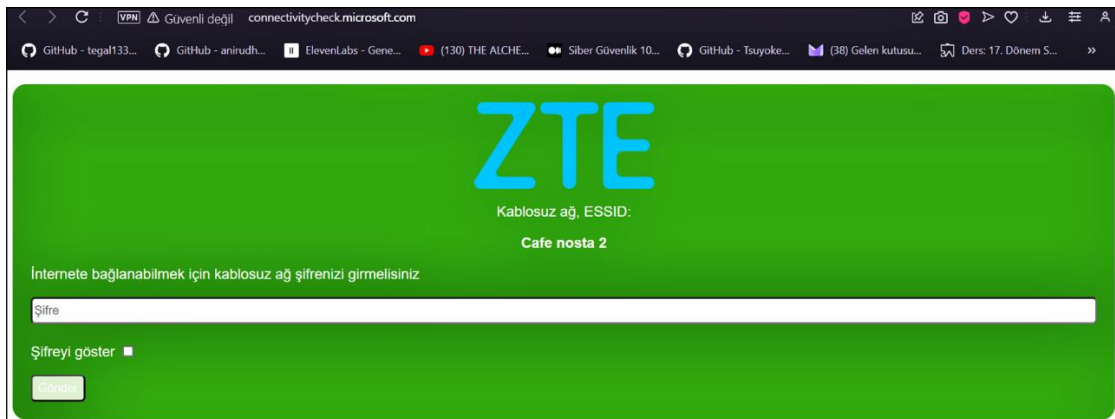
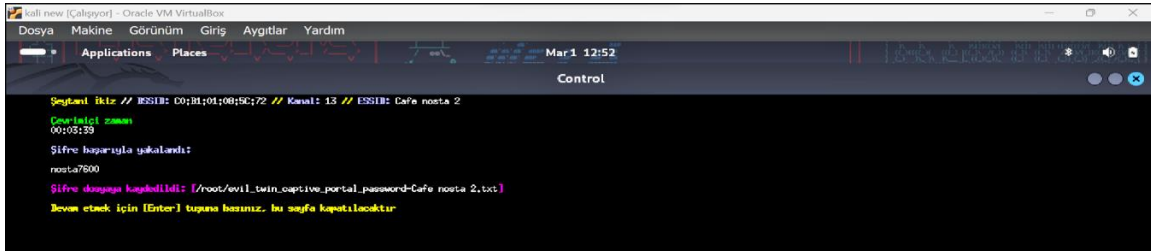


Figure 8. Configured login portal for victim connection.

Upon connection, the user will be greeted with a page prompting them to enter a specially configured WiFi password. This page can be customized to withhold internet access until the user provides the requested information (Figure 9). Additionally, even if an incorrect password is entered, internet access will not be

granted; only when the correct password is entered will the victim be granted internet access. These measures are designed to enhance information security and prevent unauthorized access.



```

koll new [Çalışıyor] - Oracle VM VirtualBox
Dosya Makine Görünüm Giriş Aygıtlar Yardım
Applications Places Mar 1 12:52
Control
Şeybeni İkiz // ESSID: D0:B1:01:00:5C:72 // Kanal: 13 // ESSID: Cafe_nosta_2
Çevrimiçi zaman: 00:03:39
Sifre başarıyla saklandı:
nosta7600
Sifre dogayla kaydedildi: [/root/evil_twin_captive_portal_password-Cafe_nosta_2.txt]
Devam etmek için [Enter] tuşuna basınız. Bu sayfa kapatılmaktadır

```

Figure 9. Demonstration of successful completion and results of Evil Twin attack.

Figure 9 shows the successful completion and results of a wireless network attack scenario. At this stage, it is evident that a user has entered a password into the fake network portal, and this entry has been captured by the attacker. Alongside a message confirming the successful entry, it is indicated that the password entered by the user has been saved to a file and reflected in the Linux terminal. This outcome demonstrates how, within the context of an Evil Twin attack, the attacker gathers and stores authentication information obtained from the target user. By convincing the user to connect to their controlled fake network and enter the network password, the attacker gains access to this information.

4 DISCUSSION

Evil Twin attacks stand out as a significant security threat in wireless networks. These types of attacks aim to capture users' information by creating fake access points. This type of attack can seriously threaten the information security of users and organizations, leading to financial losses. Therefore, it is important to develop and implement effective protection strategies against Evil Twin attacks. Hence, this study conducted a real case analysis to address the potential risks of Evil Twin attacks and the measures to be taken.

Such attacks are often carried out without users' awareness and can result in the capture of sensitive information or the deception of users. In this context, it is important for users to be aware of and implement protection strategies against Evil Twin attacks. Additionally, the effects of Evil Twin attacks on organizations and businesses should be examined. These attacks can jeopardize the reputation and

credibility of businesses and put customers' security at risk. Therefore, it is necessary for businesses to strengthen their defense strategies against Evil Twin attacks and take necessary measures to protect sensitive information.

The methods used to carry out the attack need to be evaluated in the case analysis examined in the study. Firstly, it is important that such tools are used within a legal framework. The usage of hacking tools and unauthorized access to networks are illegal in many countries and can have serious legal consequences. Therefore, it is important that these tools are used only for legal and ethical purposes. Additionally, the usage of these tools brings ethical considerations. Cybersecurity experts should respect personal privacy and security while using these tools and should not engage in unauthorized access.

Furthermore, the potential harms and consequences of using these tools should be taken into account. A step-by-step scenario has been created for the execution of Evil Twin attacks, clearly demonstrating the steps taken by the attacker to gain access to the target network. As a result of these steps, the attacker has gained unauthorized access to systems by capturing the identities of legitimate users, thereby increasing the likelihood of accessing sensitive data, seizing control of systems, and engaging in other malicious activities. However, the impact and damage of the attack can vary depending on the attacker's motivation and the security measures of the target network.

To effectively counteract evil twin attacks, it is essential to implement a comprehensive set of preventive measures and defense strategies. First, employing robust and up-to-date network security protocols and encryption methods is crucial. Network administrators should secure their networks using the latest encryption standards, such as WPA3, and encourage the use of strong, complex passwords to further enhance security. In addition to encryption, regular security vulnerability scans and penetration tests are necessary to identify and mitigate network vulnerabilities. These ongoing scans help administrators understand the evolving techniques used by attackers, enabling them to develop targeted defense strategies against threats like evil twin attacks.

Furthermore, the utilization of firewalls and network monitoring tools by both administrators and users is vital to track network traffic and detect any unusual

activities, facilitating early detection and prevention. Raising end-user awareness is equally significant in creating a multi-layered defense system. By educating users on how to recognize fake access points and avoid connecting to untrusted networks, the overall effectiveness of these preventive measures can be greatly enhanced. Security awareness training provides users with the knowledge needed to understand the risks posed by evil twin attacks and how to protect themselves accordingly.

Assessing the effectiveness of evil twin attacks in different environments is also important for understanding their potential impact in real-world situations. For example, evaluating how these attacks perform on networks using different security standards—such as WPA, WPA2, and WPA3—reveals specific vulnerabilities and indicates which protocols are more resistant. Even advanced encryption like WPA3 may be vulnerable under certain conditions, particularly due to user errors or incorrect configurations.

Acknowledging the limitations of the tools used to execute these attacks is also crucial. The dependency on specific hardware and software, especially when targeting networks with enhanced security measures, can significantly restrict the effectiveness of these attacks. The success of an evil twin attack is often influenced by the capabilities of the tools and the security measures in place within the target network, showing that both environmental and technological factors significantly affect the outcome.

Considering future advancements is essential when discussing the progression of evil twin attacks. The integration of new technologies, such as artificial intelligence and machine learning, could make these attacks harder to detect while allowing attackers to use more advanced techniques. Therefore, it is imperative to strengthen existing defense mechanisms and advance AI-driven detection methods. Such developments will ensure that defense strategies are continuously adapted to counter new and sophisticated threats.

Finally, the protection strategies presented in this study emphasize both enhancing security protocols and increasing user awareness. The adoption of advanced encryption standards and robust authentication mechanisms forms the foundation of a strong defense against evil twin attacks. Moreover, improving user awareness is equally critical—organizations should regularly provide security training

to help end-users recognize and avoid untrusted access points. Empowering users with the skills and knowledge needed to identify potential threats will significantly improve overall resilience to such attacks. These user-centered strategies, in conjunction with technical countermeasures, create a holistic approach to mitigating the risks associated with evil twin attacks.

5 CONCLUSION AND SUGGESTIONS

Evil twin attacks pose a significant cybersecurity threat to both users and companies. These attacks can compromise the identities of legitimate users, gain unauthorized access to systems, and potentially cause extensive financial and reputational damage by compromising sensitive data. The analysis conducted in this study examines a real case of evil twin attacks, focusing on the strategies employed by attackers, the analysis methods of this threat, and defense mechanisms against it.

Understanding the thought process and strategies of attackers is a critical step in preventing evil twin attacks in cyberspace. This understanding can serve as an important tool for cybersecurity experts to anticipate attackers' actions and adjust defense strategies accordingly. Firstly, understanding the motivations and objectives of attackers can help in identifying potential targets and directing their attacks. Secondly, analyzing the techniques and strategies used by attackers can help identify weaknesses in existing defense mechanisms. This is crucial for strengthening defense strategies and effectively preventing attacks. Additionally, a detailed analysis of attackers' pre-attack preparations and behavior during attacks can help cybersecurity experts improve their ability to detect and respond to attacks. These insights can contribute to the development of more effective cybersecurity strategies and the enhancement of stronger defense mechanisms against evil twin attacks in cyberspace.

To effectively mitigate the risks posed by rogue access point attacks, users must adopt a range of precautionary measures, as outlined below:

1. **Avoiding Untrusted Networks:** Users should avoid connecting to wireless networks whose authenticity cannot be verified. This is particularly pertinent

to free Wi-Fi services in public places, as these networks carry a high risk of impersonation.

2. **Verification of Access Point Identity:** Before connecting to a wireless network, users must verify the network name and identity carefully. Any unexpected or unfamiliar network name might indicate a potential attack, in which case users should refrain from connecting.
3. **Enhancing Security Through VPN Usage:** Utilizing a Virtual Private Network (VPN) encrypts internet traffic, thereby enhancing security and preventing attackers from intercepting the data. This measure is especially critical when using public networks to ensure user privacy.
4. **Disabling Automatic Connection Feature:** The automatic connection feature in devices may result in connecting to untrusted networks without the user's knowledge. Disabling this feature can prevent inadvertent connections to potentially harmful networks, thereby increasing security.
5. **Utilization of Updated Security Software and Antivirus:** Keeping security software and antivirus programs up to date is crucial for identifying and mitigating potential threats. This proactive approach strengthens the defense against malicious access points.
6. **Securing Data Using HTTPS Protocol:** Users are encouraged to use the HTTPS protocol during their internet activities to ensure data traffic is encrypted, thereby reducing the risk of sensitive information being compromised. This protocol plays a key role in safeguarding personal information such as credentials.

These measures are intended to reinforce the security of end-users against potential threats that may arise in wireless networks. By implementing such strategies, users can become more resilient to attacks such as the evil twin.

The knowledge and skills required to execute evil twin attacks necessitate expertise in the field of cybersecurity. Therefore, organizations should strengthen their defense mechanisms, provide continuous training for personnel, and regularly update security measures. Additionally, legal and ethical considerations should be

taken into account, and organizations should strive to fully comply with laws and ethical standards.

Future research should focus on developing more effective defense strategies against evil twin attacks. This requires a comprehensive research effort focused on better understanding attack methods, improving defense mechanisms, and advancing cybersecurity technologies. Moreover, increasing collaboration and information sharing can accelerate developments in cybersecurity and support organizations in creating a more secure cyber environment. In this way, organizations can establish a more secure and reliable cyber environment and minimize the impacts of cyber-attacks.

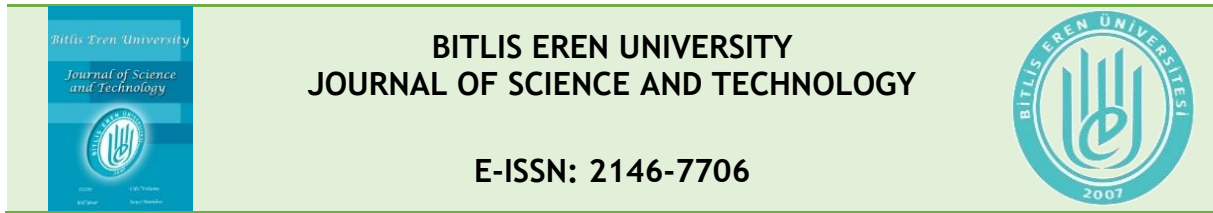
Statement of Research and Publication Ethics

The study is complied with research and publication ethics.



REFERENCES

- [1] H. Gonzales, K. Bauer, J. Lindqvist, D. McCoy, D. Sicker, "Practical defenses for evil twin attacks in 802.11," *In 2010 IEEE Global Telecommunications Conference GLOBECOM 2010* IEEE. 2010. pp. 1-6.
- [2] P. Shrivastava, J. Mohd Saalim and K. Kotaro, "EvilScout: Detection and mitigation of evil twin attack in SDN enabled WiFi." *IEEE Transactions on Network and Service Management* vol.17.1, pp. 89-102. 2020.
- [3] R. Banakh, A. Piskozub, I. Opirskyy, "Devising A Method For Detecting Evil Twin" Attacks On IEEE 802.11 Networks (Wi-Fi) With Knn Classification Model. *Eastern-European Journal of Enterprise Technologies*, vol.9, pp.123, 2023.
- [4] F. Lanze, A. Panchenko, I. Ponce-Alcaide, T. Engel, "Undesired relatives: protection mechanisms against the evil twin attack in IEEE 802.11," *In Proceedings of the 10th ACM symposium on QoS and security for wireless and mobile networks*, pp. 87-94, 2014.
- [5] L. M. da Silva, V. M. Andregretti, R. A. F. Romero, K. R. L. J. C. Branco, "Analysis and Identification of Evil Twin Attack through Data Science Techniques Using AWID3 Dataset," *In Proceedings of the 6th International Conference on Machine Learning and Machine Intelligence* pp. 128-135. 2023.
- [6] A.S. Guide, "Evil Twins: Handling Repetitions in Attack-Defense Trees," *In Graphical Models for Security: 4th International Workshop, GramSec 2017, Santa Barbara, CA, USA, August 21, 2017, Revised Selected Papers*, Springer. Vol. 10744, p. 17, 2018.
- [7] R. Muthalagu, S. Sanjay, "Evil twin attack mitigation techniques in 802.11 networks," *International Journal of Advanced Computer Science and Applications*, vol.6, pp.12, 2021.

- [8] M.S. Ahmad, S. Lutfi, and S. D. Abdullah. "Extended generic process model for analysis mitm attack based on evil twin." *Journal of Physics: Conference Series*. Vol. 1569. No. 2. IOP Publishing, 2020.
- [9] Q. Lu, H. Qu, Y. Zhuang, X.J. Lin, Y. Zhu, Y. Liu, "A passive client-based approach to detect evil twin attacks," *In 2017 IEEE Trustcom/BigDataSE/ICSS*, pp. 233-239, 2017.
- [10] A. Esser, C. Serrao, "Wi-Fi network testing using an integrated Evil-Twin framework," *In 2018 Fifth International Conference on Internet of Things: Systems, Management and Security*, IEEE. pp. 216-221, 2018.



EXERGO-ENVIRONMENTAL SUSTAINABILITY ASSESSMENTS OF ORGANIC RANKINE CYCLE PLANTS POWERED BY A TYPICAL ABANDONED OIL WELL

Larry Orobome Agberegba ¹ , Joseph Oyekale ^{2, *} 

¹Federal University of Petroleum Resources Effurun, Department of Mechanical Engineering, Nigeria, agberegba.larry@fupre.edu.ng

²Federal University of Petroleum Resources Effurun, Nigeria, oyekale.oyetola@fupre.edu.ng

* Corresponding author

KEYWORDS

Abandoned oil well retrofit
Organic Rankine Cycle
Energy Efficiency
Sustainable Energy System
Exergetic Sustainability
Exergo-environmental
Analysis

ARTICLE INFO

Research Article

DOI

[10.17678/beuscitech.1472921](https://doi.org/10.17678/beuscitech.1472921)

Received 24 April 2024

Accepted 09 December 2024

Year 2024

Volume 14

Issue 2

Pages 75-102



ABSTRACT

Economic and technical factors often force players in the oil and gas sectors to abandon oil wells with significant but minimal energy contents. To promote energy efficiency, efforts are ongoing to explore viable means of recovering such residual energy, basically as geotherms, for power generation. However, there are sparse studies in the literature that assess the exergo-environmental sustainability potentials of power generation from ORC using abandoned oil wells as the primary energy source, thereby necessitating this study.

The exergetic sustainability and exergo-environmental performance of non-recuperative and recuperative organic Rankine cycle (ORC) plants were assessed in this study for the production of electricity from abandoned oil wells. The geomechanical properties of a typical oil well in Nigeria were employed as inputs into an established COMSOL model to determine the thermal profile of the heat source. For the ORC plant, the mass, energy, and exergy balance equations defined by the Thermodynamics laws were implemented in MATLAB. Also, MATLAB was adopted for computing the exergetic sustainability and exergo-environmental metrics for the individual components and the entire system.

Results showed that the condenser exhibited the least exergo-environmental sustainability for both ORC schemes assessed, meaning that it contributed the most to energy wastages among the system components. Furthermore, results showed that the exergo-environmental impact rates of the condenser are highest in both cases. Generally, results showed that the inclusion of a recuperator would improve the exergy-based environmental sustainability of the ORC plant. Specifically, the overall rate of exergo-environmental impact would decrease from around 86 Pt/h to about 76 Pt/h, amounting to approximately 13% decrease.

1 INTRODUCTION

An essential part of the oil and gas exploration process is the drilling of wells for scooping the desired products deposited in the earth. However, the quality and quantity of crude oil and gas producible from wells diminish over time due to several geological and mechanical challenges associated with the age of oil and gas wells [1]. Close to the end of life of oil and gas wells when the water contents in the wells have increased tremendously, operators have the choice of deploying enhanced oil recovery (EOR) technologies to optimize oil and gas outputs from wells and of course the profits accruable to the company [2], [3], [4]. However, oil and gas players in several developing countries such as Nigeria consider the costs of EOR too intensive, and considering the availability of vast oil and gas reserves in other virgin fields, they tend to simply abandon depleting wells and move on to develop new ones. Consequently, huge thermal energy available in the abandoned wells is wasted, and the oil wells so abandoned without adequate decommissioning are major sources of environmental degradation. Thus, researchers have been investigating other potential uses of heat in abandoned oil and gas wells, in which case the conversion to geothermal sources for power production is at the fore [5], [6], thereby placing this study in a proper perspective.

The organic Rankine cycle (ORC) is today ubiquitous energy conversion technology that plays a critical role in the conversion of low-temperature thermal energy to electricity [7], [8], [9]. Besides the ORC, there are other methods for low-temperature conversion to useful energy, Agberegha et al. [10] proposed a novel combined-cascade steam-to-steam trigeneration cycle integrated with vapour absorption refrigeration (VAR) and district heating systems. The proposed trigeneration system incorporated a binary $\text{NH}_3\text{-H}_2\text{O}$ VAR system, emphasizing its significance in low-temperature energy systems. The VAR system achieved a cycle exergetic efficiency of 92.25% at a cooling capacity of 2.07 MW, utilizing recovered waste heat at 88 °C for district hot water. The recovered heat minimizes overall exergy destruction, enhancing thermal plant performance.

ORC is synonymous with the conventional steam Rankine cycle in its processes, differing only in the use of organic working fluid instead of water used in the steam Rankine cycle [11], [12]. Several researchers have tipped the ORC as a viable

technology for exploiting the residual thermal energy in abandoned oil wells for electricity production [13], [14], [15], [16]. However, most of the previous studies on the subject have been limited to techno-economic feasibility studies based on the First Law of Thermodynamics [17], without much recourse to the environmental aspects. Considering the potential threat that such systems could pose to the environment, it is vital to incorporate environmental assessment [18] into the technical feasibility studies of power production from abandoned oil wells using ORC plants.

Researchers have postulated exergetic approaches, derived from the 2nd Law of Thermodynamics, for integrating environmental assessment with technical analysis of energy systems, in the form of exergetic sustainability assessments [19], [20], [21] and exergo-environmental analysis [22], [23]. A few studies on ORC plants that have incorporated both the exergetic sustainability and exergo-environmental methods are summarized here. Parham et al. [24] employed the exergetic sustainability method to examine the roles of evaporator temperature on the output power of an ORC plant and hydrogen production rate from an electrolyzer in a tri-generation system using an open absorption heat transformer (OAHT) as the heat source. The authors affirmed that increasing the evaporator inlet temperature is in favor of the environment by the increase in exergetic sustainability factor and decrease in exergo-environmental impact. Abam et al. [25] adopted the exergy-based sustainability indicators to determine an optimum amongst several ORC configurations utilizing low-temperature energy sources. They reported specifically that system configuration and working fluid choice play significant roles in the sustainability of ORC plants. In another study, Abam et al. [26] used the exergetic sustainability indices to compare the performance of R245fa, R1234yf, and R1234ze when employed as working media in ORC plants. The authors again reiterated that either of the refrigerants compared could give optimal sustainability performance depending on the actual ORC configuration in focus. Also, Abam et al. [27] investigated the effects of evaporator pressure and heat source temperature on the exergetic sustainability of several ORC configurations, reporting that strong correlations exist between the varied cycle parameters and its sustainability, as would be expected. Adebayo et al. [28] identified the current density in a multi-generation energy system comprising a solid oxide fuel cell, an ORC, and an

absorption chiller as a major factor affecting exergetic sustainability and environmental impact. Specifically, the authors reported that increasing the current density would harm the sustainability of such a system. Nasruddin et al. [29] analyzed the exogoenvironmental performance of a binary geothermal ORC plant operational in Indonesia, reporting a total environmental impact of about 0.3 Pt/s for the system. Also, Alibaba et al. [30] employed the exergy-based method to investigate the impacts of a solar-geothermal ORC system on the environment. They obtained that the solar system had the highest environmental impact on the hybrid plant and that exergy destruction contributed the most to the overall environmental impact of the system. Ding et al. [31] reported the significance of working fluid leakage in the environmental impacts of ORC systems. Specifically, for R245fa, R134a, R152a, and R227ea compared in the study, the authors obtained that between 2.6% and 26% of the environmental impact is directly linked with the working fluids, between 36% and 78% of which are due to leakages. Fergani et al. [32] used the exergo-environmental method to study the optimization potentials in an ORC plant for waste heat recovery in the cement industry. They reported that from the exergo-environmental viewpoint, the heat exchangers should be optimized, for the overall improvement of the entire ORC system.

It is explicit from the foregoing that ORC can be employed to optimally produce electricity from abandoned oil wells. Also, the exergetic sustainability and the exergo-environmental methodologies are being explored widely for integrated environmental assessments of ORC plants for different applications. However, no study has been found in the literature that assessed the exergo-environmental sustainability potentials of power generation from ORC using abandoned oil wells as the primary energy source. Considering the importance of the environmental performance of ORC plants for such an application, its environmental assessment based on the Second Law of Thermodynamics is a vital research gap that is aimed to be bridged in this article. Specifically, two different ORC configurations are proposed and assessed using both the sustainability and environmental approaches derived from the Second Law. The first ORC configuration is a basic subcritical ORC without internal heat recuperation, named here as SUB ORC, while the second is a recuperative subcritical ORC plant tagged here as SUB-REGEN ORC. The tangential study objectives are:

- To quantify the exergo-environmental sustainability indices for a defined SUB ORC plant generating electricity from an abandoned oil well in Nigeria;
- To quantify the exergo-environmental sustainability indices for a defined SUB-REGEN ORC plant;
- To quantify the effects of incorporating an internal heat recuperator on the exergy-based environmental sustainability of the ORC plant for power production from an abandoned oil well.

2 MATERIALS AND METHODS

2.1 System Configurations

Thermal energy content in an abandoned oil well was considered in this study as the heat source for electricity generation by an organic Rankine cycle (ORC) power plant. Specifically, a coaxial borehole heat exchanger (BHE) was plugged into the abandoned well for heat energy exploitation and connected to the ORC power plant through its evaporator and preheater. A numerical analysis of the BHE already established in the literature [33] was adopted in this study using as input parameters the geometrical features of a typical oil well already abandoned in the oil-rich Delta State of Nigeria [34]. The main features of the BHE employed in this study are highlighted in Table 1. The temperature of the geothermal brine interfacing the ORC plant was determined from the simulation of the BHE in COMSOL as presented in [33], adapting the geometrical characteristics of the reference oil well.

The ORC plants analyzed in this study assumed two configurations: a subcritical ORC plant without internal heat recuperation, tagged here as SUB ORC, and another one with heat recuperation, dubbed in this study as SUB-REGEN ORC. As aforementioned, the ORC plant, irrespective of the configuration assumed, received the residual thermal energy exploited from the abandoned oil well through the geothermal fluid. The geothermal brine enters the evaporator of the ORC plant and exchanges heat with the organic working fluid of the ORC and the remaining thermal content of the geothermal fluid is further exchanged with the ORC plant in the preheater before the brine is re-circulated in the oil well. The fluid R236fa was considered in this study as the ORC working medium. After it has been preheated and evaporated at high pressure by the geothermal brine, the high-temperature

R236fa vapor is expanded in the turbine (turbogenerator) for electrical power production. The expanded ORC working fluid, still in a vapor state, is then condensed back to liquid in the condenser for the non-recuperative ORC configuration (SUB ORC) by discharging its thermal energy to a heat sink. In the case of the recuperative ORC configuration (SUB-REGEN ORC), the heat of the expanded working fluid vapor is recovered internally within the cycle by the recuperator, for the initial preheating of the working fluid at the pump exit, after which the expanded vapor is condensed to a liquid. In both cases, the liquid working fluid leaving the condenser is pressurized in the pump to increase pressure from the lower to the upper cycle pressure, and the cycle repeats. Compressed air was considered as the heat sink in both cases due to the scarcity of water in the location of the abandoned oil well being exploited. The organic working fluid R236fa was selected based on its good thermal stability, low environmental impact, and ultimately its common application in practical ORC systems [35], [36], [37]. The SUB ORC and SUB-REGEN ORC configurations are illustrated in Figure 1a and 1b.

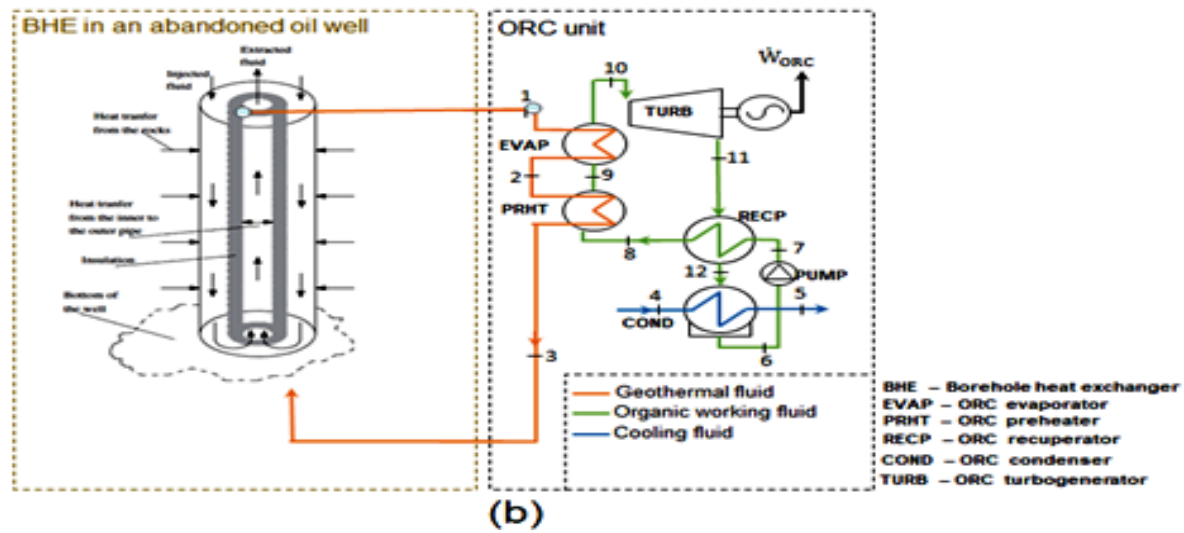
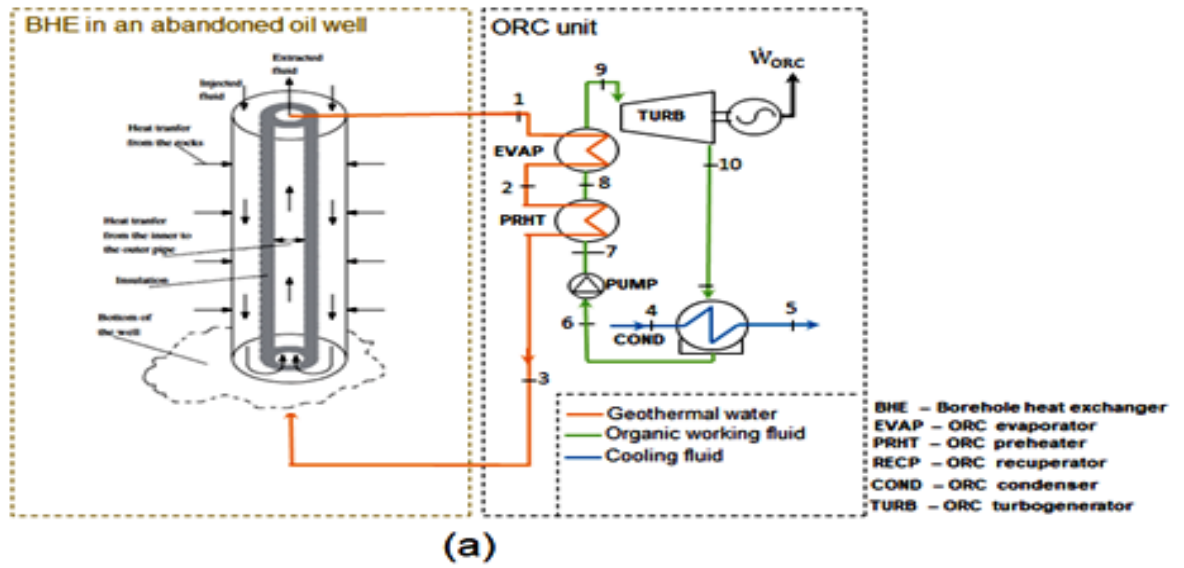


Figure 1. The non-recuperative and recuperative ORC units.

2.2 Exergetic Sustainability Analysis

To assess the sustainability of energy systems from the exergy perspective [20], comprehensive exergy analysis is first required, which entails each component and the overall system satisfying the mass and energy balance equations mandated by the First Law of Thermodynamics and the exergy balance equation enforced by the Second Law, as expressed in equations 1, 2, and 3, respectively:

$$\sum \dot{m}_i = \sum \dot{m}_o \quad (1)$$

$$\sum \dot{m}_i h_i + \dot{Q} = \sum \dot{m}_o h_o + \dot{W} \quad (2)$$

$$\sum \dot{m}_i e_i + \dot{Q} \left(1 - \frac{T_a}{T_c}\right) = \sum \dot{m}_o e_o + \dot{W} + \dot{i} \quad (3)$$

where T symbolizes the temperature at any given state, e symbolizes specific exergy, \dot{i} for any component denotes the rate of exergy destroyed, \dot{Q} symbolizes heat flow, \dot{W} is the rate of workflow, h symbolizes enthalpy per unit mass, and \dot{m} is the rate of mass flow of the working fluid.

All the parameters with subscript i account for the inlet flow into a component while those with o account for exit flows. The ambient parameters are symbolized by subscript a while those for the surface of the respective components are denoted by c .

The potential exergy (e_{pe}), chemical exergy (e_{ch}), kinetic exergy (e_{ke}), and physical exergy (e_{ph}), are the four primary components that make up the specific exergy, fundamentally (T. J. Kotas, 1985). Analysis of most energy systems fixed in position do not include the kinetic and potential exergy components, and most systems without actual chemical reactions - like the ORC systems being studied herein - have zero chemical exergy. Therefore, the physical exergy sufficiently models the total exergy per unit mass herein, defined by:

$$e_{ph} = (h-h_a) - T_a(s-s_a) \quad (4)$$

where for each stream, defined by distinct thermal-fluid properties, s connotes entropy per unit mass. Table 1 reports, for the plants being investigated herein, the fundamental design elements.

Table 1. Abandoned oil well and ORC basic design features.

Abandoned oil well and BHE		ORC unit	
Well head	4500 m	Working fluid	R236fa
BHE tube radius	3.8 cm	Heat sink	Air
BHE annulus radius	8.9 cm	Net electrical power	Optimized
BHE thickness	1 cm	Nominal input thermal power	Decision variable
Brine temperature	155°C	Nominal HTF flow rate	Decision variable
		Isentropic efficiency - pump	0.80
		Motor efficiency - pump	0.98
		Isentropic efficiency - turbine	0.85
		Electromechanical efficiency	0.92
		Mechanical efficiency - cooling fan	0.60
		Pinch point temperature difference	5 °C

2.3 Exergy-Based Sustainability Performance Metrics

This study compared the two ORC configurations using four exergy-based sustainability indicators, which are explained below [38]. In any component k , product exergy (\dot{E}_P) to fuel exergy (\dot{E}_F) ratio defined the exergy efficiency (η_{ex}). The net exergy used on the component defines its fuel exergy; on the other hand, the net exergy generated by the component is its product exergy. One of the fundamental propositions of the 2nd Law of Thermodynamics is that the useful energy (exergy) entering and exiting a component (k) cannot be equal because all real systems are irreversible, meaning that some exergy must be destroyed in the component. The fuel exergy and product exergy per unit mass have been defined for each of the components of the systems under investigation herein, as highlighted in Tables 2 for the SUB ORC and Table 3 for the SUB-REGEN ORC configurations.

One popular performance indicator of exergy-based environmental sustainability of energy systems is the Exergy Sustainability Index (ESI), expressed by:

$$ESI = \frac{\eta_{ex}}{1 - \eta_{ex}} \quad (5)$$

A component bears greater weight in the overall sustainability of the system the higher its ESI value. Conversely, a component's environmental impact increases with decreasing ESI value. Consequently, the Environmental Effect Factor (EEF), which is yet a common performance metric for exergy-based sustainability of a system, was calculated herein by inverting the ESI.

To further enhance exergy-based sustainability, a different metric was employed to specify the amount of exergy losses and destruction in a particular component k that could be recovered. Here, it is known as the exergy-based improvement potential rate (IPR), and its computation is as follows:

$$IPR = (1 - \eta_{ex})(\dot{E}_F - \dot{E}_P) \quad (6)$$

The fourth metric, the Exergetic Recoverability Ratio (RECR), was defined for each component k as:

$$RECR = \frac{IP}{\dot{E}_F} \quad (7)$$

2.4 Exergo-Environmental Analysis

The exergo-environmental approach combines life cycle assessment (LCA) and theoretical exergy principles to measure the environmental implications of irreversibility and the usable energy in and out of a system and accompanying components. Herein, the LCA approach was used in addition to the traditional exergy analysis, as previously mentioned, to evaluate the environmental effects of the various ORC components. These were then combined in accordance with the conventional exergo-environmental methodology's definition [22].

The standard life cycle assessment approach, which consists of four major stages and is used to investigate the environmental impacts of a product or process over its entire life cycle, was applied to characterise the environmental impacts of the ORC plants [39]. The first stage involves defining the study goal and scope, as well as the effect categories, characterization elements, and boundary of analysis. A life cycle inventory study, which estimates all material and energy fluxes into and out of a component or system, is included in the second stage. Impact evaluations are conducted in the third stage with the use of suitable impact assessment techniques, many of which are integrated into Life Cycle Assessment (LCA) software. In the final step, the findings from the earlier phases are analysed to estimate the system's environmental impact.

Exergo-environmental analysis necessitates assigning environmental implications to each exergy stream for the system's individual components and as a whole. Thus, a point-based environmental impact method for energy streams is frequently employed in addition to objective and scope definition and inventory analysis based on the system model. The environmental impact of component/system streams was assigned in this study using the eco-indicator-99 (EI-99) impact identifier. The EI-99 technique uses a hierarchical weighting system to create a single environmental index for processes and products, correlated with key harm aspects: natural resources, human health, and ecosystem quality [40]. The approach defines indices in millipoints (mPts) or points (Pts) for various processes and products, based on the LCA international standards. The more environmental harm a process or system component causes, the higher the EI-99 points that are awarded for that exergy stream or component. Following the assignment of

environmental impacts in points to system components/streams for the exergy-based Life Cycle Assessment (LCA) of the system, the exergo-environmental variables are computed.

Meyer et al. [22], developed the exergo-environmental approach and suggested a balance equation that is similar to the exergoeconomic cost balance equation. Equations 8 and 9, which establish the component-level balancing equation, are the foundation of exergo-environmental analysis nowadays.

$$\sum B_i + B_q + (Y + B^{PF}) = \sum B_o + B_w \quad (8)$$

$$\sum b_i E_i + b_q Q + (Y + B^{PF}) = \sum b_o E_o + b_w W \quad (9)$$

with B denoting environmental impact rate, obtainable by multiplying the environmental impact per unit mass of a stream (b, Pts/kWh) with its exergy rate (E, kW), subscripts q and w denote specific heat and work flow to and from a component, respectively, B^{PF} symbolizes the contribution of pollutants formed in a component to its environmental impact rate, and aggregating the impact rates resulting from component's construction Y^{CO} , maintenance/operation, Y^{OM} , and end-of-life disposal, Y^{DI} , would yield Y (component's environmental impact rate). Also, B^{PF} is defined for each component as:

$$B^{PF} = \sum_n b_n^{PF} (\dot{m}_{n,out} - \dot{m}_{n,in}) \quad (10)$$

with b_n^{PF} representing the environmental impact per unit mass emanating from pollutant n produced by a component (Pts/kg), with $\dot{m}_{n,in}$ and $\dot{m}_{n,out}$ denoting inlet and exit mass flow rates of the pollutant, respectively.

The exergo-environmental balance equations for the SUB ORC and SUB-REGEN ORC components are equally defined respectively in Tables 2 and 3. Based on the weight and material composition of each component, the environmental consequences were computed in EI-99 points. Applying the inventory analysis and manufacturer specifications for the corresponding plant units, theecoinvent database was utilised to calculate the weight and composition of the ORC components/sub-units[41], [42]. Auxiliary equations were defined using the product-fuel (P-F) rule, supplemented by the environmental balance equations, to arrive at the definitions for environmental impact per unit mass (b) for the individual

thermodynamic streams of the system [43], highlighted also in Tables 2 and 3 for each of the ORC configurations being investigated. The final step involves setting up all the auxiliary and balance equations for all system components and solving them simultaneously, as a stream's specific cost would be determined using the popular specific exergy costing (SPECOC) method of exergoeconomic analysis [44].

2.5 Exergo-Environmental Evaluation Parameters

The total exergo-environmental impact rate (BRT), exergo-environmental factor (f_b), specific exergo-environmental impact relative difference (r_b), exergo-environmental impact per unit energy produced (EIE), exergo-environmental impact rate due to irreversibility in system component (\dot{B}_D), exergo-environmental impact per unit fuel consumed (b_f), and the exergo-environmental impact per unit product exergy (b_p) were employed herein to compare the two ORC configurations. The appendix defines the previously described exergo-environmental evaluation parameters for any system component k.

When the values for b have been determined for all thermodynamic streams, the P-F ruled aided the calculations of the exergo-environmental impact rates for fuel ($B_{f,k}$) and product ($B_{p,k}$). Once more, subtracting the fuel and product exergy rates for any component k would yield the irreversibility there in (I_k).

Table 2. SUB ORC components - definitions of fuel and product, exergo-environmental rate balance, and auxiliary equations.

Specific component/Abbreviation	Fuel exergy	Product exergy	Exergo-environmental rate balance equation	Auxiliary equation
Evaporator (EVAP)	$\dot{E}_1 - \dot{E}_2$	$\dot{E}_9 - \dot{E}_8$	$\dot{B}_1 + \dot{B}_8 + \dot{Y}_{EVAP}$ $= \dot{B}_2 + \dot{B}_9$	$b_1 = b_2 = 0.0425$ Pt/kWh [45]
ORC preheater (PRHT)	$\dot{E}_2 - \dot{E}_3$	$\dot{E}_8 - \dot{E}_7$	$\dot{B}_2 + \dot{B}_7 + \dot{Y}_{PRHT}$ $= \dot{B}_3 + \dot{B}_8$	$b_2 = b_3$
Condenser (COND)	$\dot{E}_{10} - \dot{E}_6 + \dot{W}_{FAN}$	$\dot{E}_5 - \dot{E}_4$	$\dot{B}_{10} + \dot{B}_4 + \dot{B}_{W,F}$ $+ \dot{Y}_{COND} = \dot{B}_5 + \dot{B}_6$	$b_4 = 0; b_{10} = b_6$
Pump (PUMP)	\dot{W}_{PUMP}	$\dot{E}_7 - \dot{E}_6$	$\dot{B}_6 + \dot{B}_{w,p} + \dot{Y}_{PUMP}$ $= \dot{B}_7$	$b_{w,p} = b_{w,T} = b_{w,F}$
Turbine (TURB)	$\dot{E}_9 - \dot{E}_{10}$	\dot{W}_{TURB}	$\dot{B}_9 + \dot{Y}_{TURB}$ $= \dot{B}_{w,T} + \dot{B}_{10}$	$b_9 = b_{10}$

Table 3. SUB-REGEN ORC components - definitions of fuel and product, exergo-environmental rate balance, and auxiliary equations.

Component (abbreviation)	Fuel exergy	Product exergy	Exergo-environmental rate balance equation	Auxiliary equation
Evaporator (EVAP)	$\dot{E}_1 - \dot{E}_2$	$\dot{E}_{10} - \dot{E}_9$	$\dot{B}_1 + \dot{B}_9 + \dot{Y}_{EVAP}$ $= \dot{B}_2 + \dot{B}_{10}$	$b_1 = b_2 = 0.0425$ Pt/kWh[45]
ORC preheater (PRHT)	$\dot{E}_2 - \dot{E}_3$	$\dot{E}_9 - \dot{E}_8$	$\dot{B}_2 + \dot{B}_8 + \dot{Y}_{PRHT}$ $= \dot{B}_3 + \dot{B}_9$	$b_2 = b_3$
Condenser (COND)	$\dot{E}_{12} - \dot{E}_6$ $+ \dot{W}_{FAN}$	$\dot{E}_5 - \dot{E}_4$	$\dot{B}_{12} + \dot{B}_4 + \dot{B}_{W,F}$ $+ \dot{Y}_{COND}$ $= \dot{B}_5 + \dot{B}_6$	$b_4 = 0; b_{12} = b_6$
Pump (PUMP)	\dot{W}_{PUMP}	$\dot{E}_7 - \dot{E}_6$	$\dot{B}_6 + \dot{B}_{w,p}$ $+ \dot{Y}_{PUMP} = \dot{B}_7$	$b_{w,p} = b_{w,T} = b_{w,F}$
Recuperator (RECP)	$\dot{E}_{11} - \dot{E}_{12}$	$\dot{E}_8 - \dot{E}_7$	$\dot{B}_{11} + \dot{B}_7 + \dot{Y}_{RECP}$ $= \dot{B}_8 + \dot{B}_{12}$	$b_{11} = b_{12}$
Turbine (TURB)	$\dot{E}_{10} - \dot{E}_{11}$	\dot{W}_{TURB}	$\dot{B}_{10} + \dot{Y}_{TURB}$ $= \dot{B}_{w,T} + \dot{B}_{11}$	$b_{11} = b_{10}$

3 RESULTS AND DISCUSSION

3.1 Results of Exergy-based Sustainability and Exergo-environmental Assessment for The Non-recuperative ORC Scheme

The basic exergy and exergo-environmental properties obtained for each state of the SUB ORC configuration are highlighted in Table 4. The pressure and temperature parameters derived directly from the design of the ORC plant, leading also to the determination of the exergy rate. The specific exergo-environmental rate (b) values were obtained by solving simultaneously the exergo-environmental balance and auxiliary equations for all the system components as aforementioned. The multiple of b with the exergy rate at each thermodynamic state gave the exergo-environmental rate (\dot{B}) following the model defined above in section 2.

Table 4. State exergy and exergo-environmental data for the SUB ORC configuration.

Stream No	Working substance	Temperature (K)	Pressure (MPa)	Exergy rate (kW)	b (Pt/kWh)	\dot{B} (Pt/h)
1	Geothermal brine	428.15	0.84	2832.5	0.043	120.4
2	Geothermal brine	400.50	0.84	1836.7	0.043	78.1
3	Geothermal brine	325.03	0.84	165.8	0.043	7.0
4	Air	298.15	0.1	0	0	0
5	Air	303.15	0.1	5.0	8.835	44.2
6	R236fa	303.15	0.32	1130.1	0.054	60.5
7	R236fa	304.73	2.88	1269.6	0.059	75.3
8	R236fa	392.84	2.88	2704.0	0.054	146.9
9	R236fa	393.84	2.88	3561.0	0.054	190.7
10	R236fa	317.56	0.32	1338.8	0.054	71.7

The main parameters used for the exergetic sustainability assessments are highlighted in Table 5 for the SUB ORC components. As can be seen, the exergetic sustainability index is lowest in the condenser and highest in the evaporator. The low sustainability of the condenser is associated with high exergy destruction resulting from the use of air as the heat sink. The same reason can be given for the high environmental effect factor obtained in the condenser, which is again the worst among the ORC system components. It is however obtained that about 717 kW of the irreversibility in the condenser can be recovered, amounting to about 99% of the fuel exergy entering the component. For the components with a relatively higher sustainability index and lower environmental effect factor such as the evaporator, preheater, and turbine, results showed that only about 2% of irreversibilities could be recovered in each. Thus, the higher the ESI of a component, the lower its EEF, and the lesser the need for structural adjustment to it for the improvement of the overall ORC plant.

Table 5. Results of exergy-based sustainability analysis results for the SUB ORC system.

Component	\dot{E}_f (kW)	\dot{E}_p (kW)	\dot{E}_D (kW)	ε (%)	ESI	IPR (kW)	EEF	RECR
Condenser	727.3	5.0	722.3	0.69	0.007	717.3	144.25	0.99
Evaporator	995.8	856.9	138.9	86.06	6.17	19.4	0.16	0.02
ORC reheater	1670.9	1434.5	236.4	85.85	6.07	33.5	0.16	0.02
Pump	233.9	139.6	94.3	59.65	1.48	38.1	0.68	0.16
Turbine	2222.2	1881.1	341.1	84.65	5.52	52.3	0.18	0.02

Similarly, the main exergo-environmental parameters are reported in Table 6 for each component of the SUB ORC plant. As can be seen, the exergo-environmental impact rate due to irreversibility is highest in the condenser still, as would be expected, followed by the turbine, preheater, pump, and evaporator. Adding the exergo-environmental impacts resulting from the construction and operation of each of the components (\dot{Y}) to those resulting from irreversibility gave the total exergo-environmental rate (**BRT**). The values of \dot{Y} for most of the components were obtained to be much lower relative to those of \dot{B}_D , such that the position of each component on the \dot{B}_D column in Table 6 is almost the same as on the one for **BRT**, except in the turbine where the \dot{Y} is highest. Also, results showed that the condenser yielded the highest of about 39 exergo-environmental points for each MW of electricity generated by the ORC plant, while the pump yielded the least of about 5 points. Additionally, the exergo-environmental factor defined for the system components showed that environmental impacts due to component construction and pollutant emissions are insignificant in the condenser, turbine, and the pump, compared to impacts due to irreversibility. However, the environmental effects of construction should be reckoned with in the evaporator and preheater where the highest f_b values were obtained at 19% and 5.6%, respectively. Additionally, the product exergy in the condenser contributes substantially to its exergo-environmental effect resulting in a very high value of r_b .

Table 6. Results of the exergo-environmental analysis for the SUB ORC system.

Component	b_f (Pt/kWh)	b_p (Pt/kWh)	\dot{B}_D (Pt/h)	\dot{Y} (Pt/h)	BRT (Pt/h)	EIE (Pts/kWh)	f_b (%)	r_b
Condenser	0.061	8.84	43.69	0.24	43.93	0.039	0.55	145.0
Evaporator	0.043	0.051	5.90	1.41	7.31	0.007	19.0	0.20
ORC preheater	0.043	0.050	10.05	0.60	10.65	0.009	5.60	0.17
Pump	0.063	0.11	5.97	0.003	5.97	0.005	0.051	0.68
Turbine	0.054	0.063	18.26	0.08	18.34	0.016	0.41	0.18

3.2 Results of The Exergy-based Sustainability and Exergo-environmental Analyses for The Recuperative ORC Scheme

The parameters employed for the exergo-environmental analysis in this case are reported in Table 7 for each thermodynamic state of the SUB-REGEN ORC

configuration, obtained from design and resulting from the definitions given earlier for the featured parameters. It should be observed that the proximity in the design criteria employed for the SUB ORC and the SUB-REGEN ORC made Table 5 and Table 7 quite similar. The main differences between the two tables are direct consequences of the introduction of an additional heat exchanger serving as the recuperator in the SUB-REGEN ORC configuration.

Table 7. State exergy and exergo-environmental data for the SUB-REGEN ORC scheme.

Stream No	Working substance	Temperature (K)	Pressure (MPa)	Exergy rate (kW)	b (Pt/kWh)	\dot{B} (Pt/h)
1	Geothermal brine	428.15	0.84	2832.5	0.043	120.4
2	Geothermal brine	400.50	0.84	1836.7	0.043	78.0
3	Geothermal brine	329.15	0.84	211.4	0.043	9.0
4	Air	298.15	0.1	0	0	0
5	Air	303.15	0.1	5.0	6.757	33.8
6	R236fa	303.15	0.32	1130.1	0.054	60.6
7	R236fa	304.73	2.88	1269.6	0.059	75.4
8	R236fa	310.41	2.88	1285.4	0.060	77.5
9	R236fa	392.84	2.88	2704.0	0.054	147.1
10	R236fa	393.84	2.88	3561.0	0.054	190.9
11	R236fa	317.56	0.32	1338.8	0.054	71.8

The exergetic sustainability performance metrics are reported in Table 8 for the SUB-REGEN ORC components. Again, results showed that the ESI is lowest in the condenser at less than 1%, and of course with the highest EEF of about 110. However, about 98% of the fuel exergy destroyed in the condenser can be recovered, making it the main component to be focused on for the overall improvement of the ORC plant. The highest ESI is recorded in this case in the preheater, resulting also in the least EEF. Generally, the components of the SUB-REGEN ORC plant can be ranked in descending order of sustainability as Preheater, evaporator, turbine, recuperator, pump, and condenser.

Table 8. Results of the exergy-based sustainability analysis for the SUB-REGEN ORC system.

Component	\dot{E}_f (kW)	\dot{E}_p (kW)	\dot{E}_D (kW)	ε (%)	ESI	IPR (kW)	EEF	RECR
Condenser	557.80	5.00	552.80	0.90	0.009	547.9	110.41	0.98
Evaporator	995.8	856.9	138.9	86.06	6.171	19.4	0.16	0.02
ORC preheater	1625.3	1418.6	206.6	87.29	6.865	26.3	0.15	0.02
Pump	233.9	139.6	94.3	59.66	1.479	38.1	0.68	0.16
Recuperator	25.5	15.8	9.7	61.97	1.630	3.7	0.61	0.14

Furthermore, the exergo-environmental parameters are reported in Table 9 for the SUB-REGEN ORC configuration. Again, the condenser contributed the most to the exergo-environmental impact of the ORC system due to high irreversibility therein, leading also to the highest BRT of 33.5 Pt/h. It is noteworthy that the least BRT of 1.2 Pt/h is recorded in the newly introduced component, the recuperator, signifying that its addition should not have an adverse environmental impact on the ORC plant. The highest exergo-environmental impact of about 26 points was obtained in the condenser for the ORC plant generating 1 MW of electrical energy, and the least of about 0.9 points was obtained in the recuperator. Additionally, the recuperator recorded the highest f_b , implying that most of the little impacts it has on the environment resulted from the component's construction and might not be avoidable. In this regard, the pump and the condenser showed the worst exergo-environmental factor values. Here too, the product exergy contributed substantially to the environmental effects of the condenser; the effects in all other components are due majorly to the fuel exergy.

Table 9. Results of the exergo-environmental analysis for the SUBREGEN ORC system.

Component	b_f (Pt/kWh)	b_p (Pt/kWh)	\dot{B}_D (Pt/h)	\dot{Y} (Pt/h)	BRT (Pt/h)	EIE (Pt/kWh)	f_b (%)	r_b
Condenser	0.060	6.76	33.29	0.24	33.53	0.026	0.72	111.21
Evaporator	0.043	0.051	5.90	1.41	7.31	0.006	19.31	0.20
ORC preheater	0.043	0.049	8.78	0.60	9.38	0.007	6.40	0.16
Pump	0.064	0.11	5.99	0.0030	5.99	0.005	0.051	0.68
Recuperator	0.054	0.13	0.52	0.68	1.20	0.0009	56.53	1.41
Turbine	0.054	0.064	18.44	0.076	18.51	0.014	0.041	0.18

3.3 Exergetic Sustainability Implications of The Integration of a Recuperator

The main impacts of adopting a recuperative ORC configuration (SUB-REGEN ORC) over the non-recuperative one (SUB ORC) are reported in this section using selected exergetic sustainability and exergo-environmental parameters.

The exergetic sustainability index (ESI) values are compared in Figure 2 for the SUB ORC and SUB-REGEN ORC configurations, at component and system levels. Results showed that a switch from the SUB ORC to the SUB-REGEN ORC would increase the ESI of the ORC plant by about 17%, from about 1.2 in the SUB ORC to around 1.4 in the SUB-REGEN ORC. As can be seen, the preheater is the main component that contributed to the increase in ESI for the SUB-REGEN ORC configuration, apart from the recuperator which is added entirely. The ESI is infinitesimally small in the condenser, the reason it is insignificant in Figure 2.

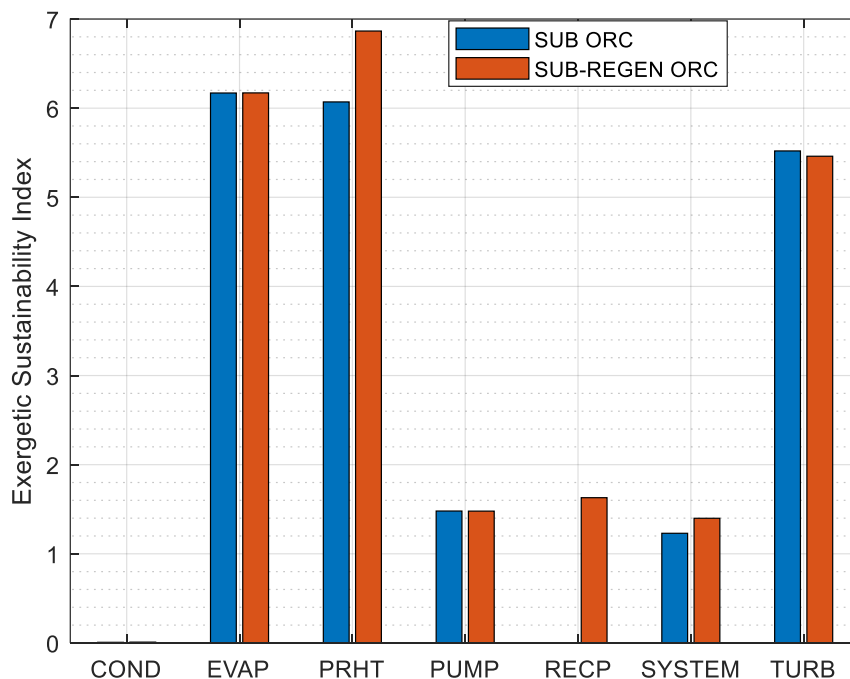


Figure 2. Exergy sustainability index (ESI) comparison for the SUB ORC and SUB-REGEN ORC configurations.

Also, the effects of introducing a recuperator on the recoverability ratio in the ORC components and the system as a whole are illustrated in Figure 3. Results showed that more opportunity exists for overall sustainability improvement in the SUB ORC system than in the SUB-REGEN ORC configuration. Specifically, the use of

the SUB-REGEN ORC configuration reduced RECR by about 7%, from about 0.45 to about 0.42. In this case, the effect is substantially due to the introduction of the recuperator which improved the exergetic performance of the SUB-REGEN ORC plant. As can be seen at the component level, the RECR values are almost the same for the two ORC configurations.

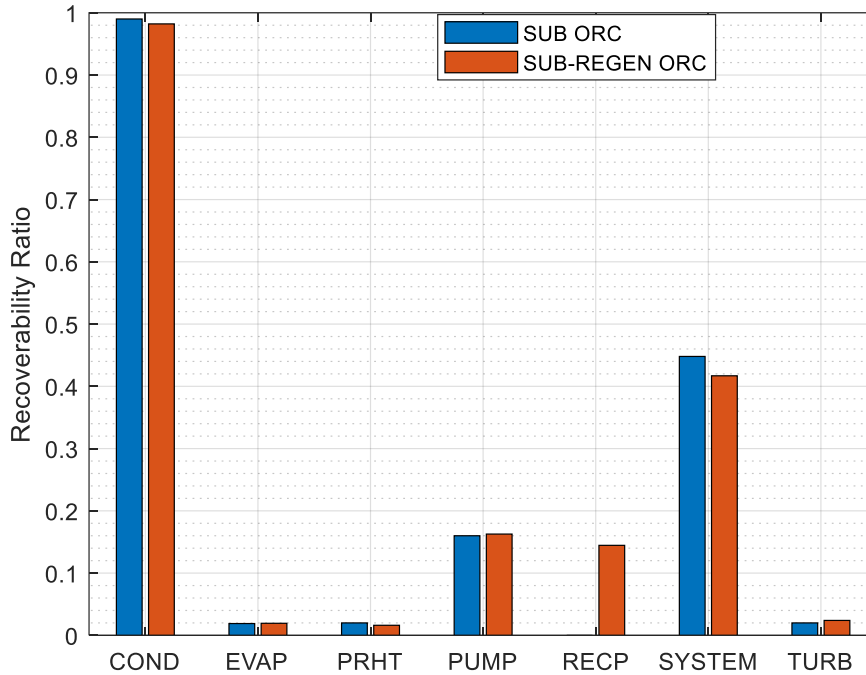


Figure 3. Comparison of recoverability ratios (RECR) for the SUB ORC and SUB-REGEN ORC configurations.

Furthermore, Figure 4 shows the impacts of the switch from the SUB ORC to the SUB-REGEN ORC configurations on the EIE. Results showed that the environmental impact of electricity is improved by about 0.02 Pts/kWh in the SUB-REGEN ORC configuration due to the improvement in the condenser and slightly in the evaporator, preheater, and turbine.

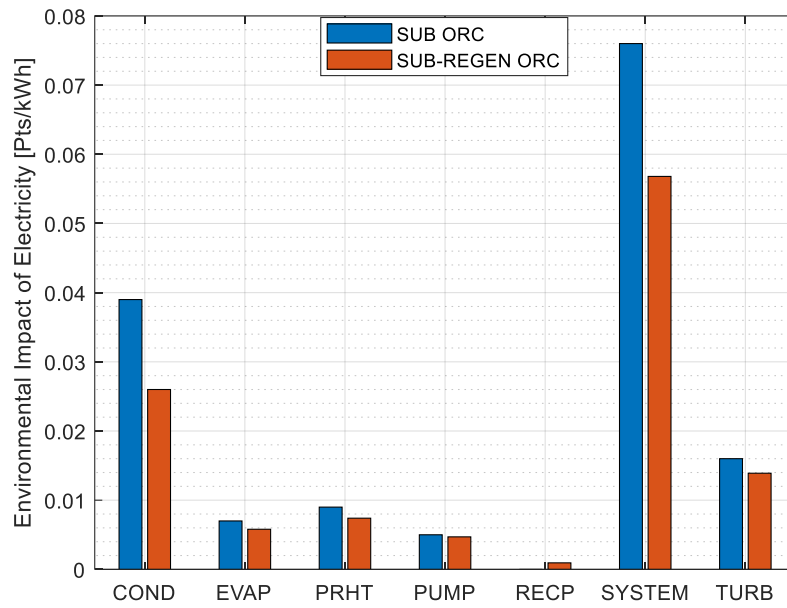


Figure 4. The environmental impact of electricity (EIE) comparison for the SUB ORC and SUB-REGEN ORC systems.

Lastly, the implication of the results in Figure 5 is that the total exergo-environmental rate can be reduced in the SUB-REGEN ORC plant by about 10 Ptis/h, amounting to about a 13% decrease in the environmental impact. As can be seen, the introduction of the recuperator contributed very little to this effect; the condenser showed the highest reduction at the component level, followed by the preheater. The effects appear insignificant in the other system components.

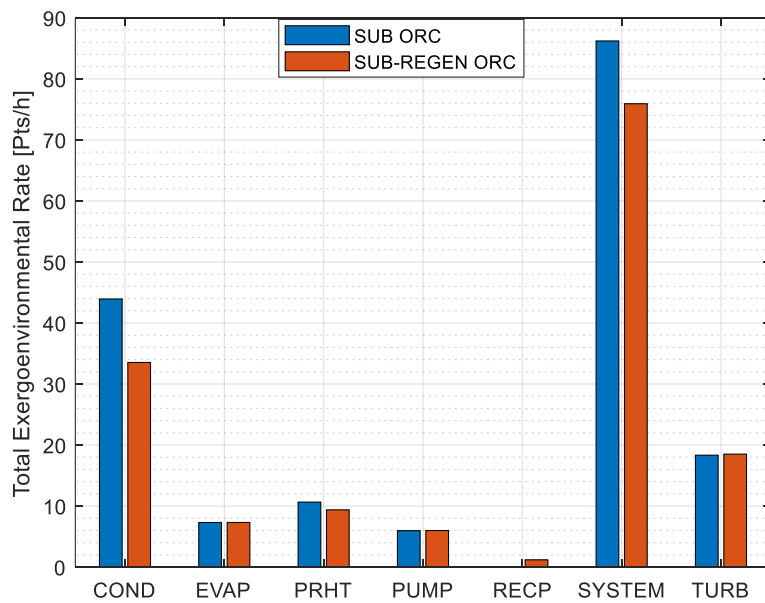


Figure 5. Comparison of total exergo-environmental rate (BRT) for the SUB ORC and SUB-REGEN ORC configurations.

4 CONCLUSIONS

The possibilities of producing electricity with organic Rankine cycle (ORC) plants from residual thermal energy in abandoned oil wells were assessed in this study using exergy-based environmental sustainability performance metrics. A lot of previous studies had tipped the ORC to be techno-economically feasible for energy generation from abandoned oil wells, but the environmental performance of such systems is not feasible in the state-of-the-art. Thus, exergy-based sustainability and exergo-environmental approaches were used herein for performance comparison of non-recuperative (SUB ORC) and recuperative subcritical ORC (SUB-REGEN ORC) configurations for the aforementioned application. The design of the ORC plants was implemented in MATLAB by solving the mass, energy, and exergy balance equations imposed by the First and Second Laws of Thermodynamics. Furthermore, the exergy-based sustainability and exergo-environmental performance metrics were assessed first for each of the two ORC configurations, followed by comparative analysis to substantiate the potential effects on the environment for choosing one ORC configuration over the other. The main results obtained from the study are:

- For the SUB ORC, the condenser showed the lowest exergetic sustainability index of 0.007 due to high irreversibility, and the evaporator had the highest sustainability index of 6.17. However, about 99% of the irreversibility in the condenser can be recovered by structural optimization, while only about 2% is achievable in most of the other components. Additionally, the exergo-environmental results showed that the condenser contributed the highest environmental impact to the SUB ORC plant at about 44 Pt/h, amounting to about 39 Pts for each 1 MW of electrical power the plant generates;
- Also, for the SUB-REGEN ORC, the condenser had the highest exergetic sustainability index which has increased to 0.009, and the preheater recorded the highest sustainability index of about 6.9. For the exergo-environmental assessment, results showed that the impact of the condenser could be reduced to 33.5 Pt/h, amounting to about 26 Pt for 1 MW of electricity produced by the ORC plant;
- The comparative analysis results showed that incorporating a recuperator into the ORC plant would increase the exergetic sustainability index of the

ORC plant by about 17%, from about 1.2 in the SUB ORC to around 1.4 in the SUB-REGEN ORC; and reduce RECR by about 7%, from about 0.45 in the SUB ORC to about 0.42 in the SUB-REGEN ORC; and improve the environmental impact of electricity by about 0.02 Pts/kWh; and reduce the overall exergo-environmental impact rate by approximately 13%, from about 86 Pts/h in the SUB ORC to around 76 Pts/h in the SUB-REGEN ORC.

In sum, the use of a recuperative ORC configuration would provide a more environmentally sustainable solution than a non-recuperative one, to produce electricity from abandoned oil wells.

Conflict of Interests

The corresponding author states, on behalf of all authors, that there is no competing interest.

Authors Contributions

J. Oyekale conceived the study and carried out the analysis. He also drafted the first version of the manuscript. Larry O. Agbergha assisted in the analysis and wrote the revised version of the manuscript.

Acknowledgement

The authors appreciate the good efforts of the reviewers and editorial staff for facilitating the review process of the manuscript.

Statement of Research and Publication Ethics

The study complies with research and publication ethics.

REFERENCES

- [1] A. A. Kassem, S. Sen, A. E. Radwan, W. K. Abdelghany, and M. Abioui, "Effect of Depletion and Fluid Injection in the Mesozoic and Paleozoic Sandstone Reservoirs of the October Oil Field, Central Gulf of Suez Basin: Implications on Drilling, Production and Reservoir Stability," *Natural Resources Research*, vol. 30, no. 3, pp. 2587-2606, 2021, doi: 10.1007/s11053-021-09830-8.

- [2] S. Jiang, Y. Li, F. Wang, H. Sun, H. Wang, and Z. Yao, "Review article A state-of-the-art review of CO₂ enhanced oil recovery as a promising technology to achieve carbon neutrality in China," *Environ Res*, vol. 210, no. February, p. 112986, 2022, doi: 10.1016/j.envres.2022.112986.
- [3] A. Talebi, A. Hasan-zadeh, Y. Kazemzadeh, and M. Riazi, "Journal of Petroleum Science and Engineering A review on the application of carbonated water injection for EOR purposes: Opportunities and challenges," *J Pet Sci Eng*, vol. 214, no. March, p. 110481, 2022, doi: 10.1016/j.petrol.2022.110481.
- [4] S. A. C. Natalya, G. T. M. Kadja, N. J. Azhari, M. Khalil, and A. T. N. Fajar, "FlatChem Two-dimensional (2D) nanomaterials for enhanced oil recovery (EOR): A review," *FlatChem*, vol. 34, no. June, p. 100383, 2022, doi: 10.1016/j.flatc.2022.100383.
- [5] D. S. E. Wiktorski and M. R. T. A. Basmoen, "Review and investigations on geothermal energy extraction from abandoned petroleum wells," *J Pet Explor Prod Technol*, vol. 9, no. 2, pp. 1135-1147, 2019, doi: 10.1007/s13202-018-0535-3.
- [6] J. Oyekale and E. Emagbetere, "19 - Pragmatic steps to the revitalization of abandoned oil and gas wells for geothermal applications," Y. Noorollahi, M. N. Naseer, and M. M. B. T.-U. of T. P. of A. W. Siddiqi, Eds., Academic Press, 2022, pp. 389-403. doi: <https://doi.org/10.1016/B978-0-323-90616-6.00019-1>.
- [7] B. F. Tchanche, Gr. Lambrinos, A. Frangoudakis, and G. Papadakis, "Low-grade heat conversion into power using organic Rankine cycles - A review of various applications," *Renewable and Sustainable Energy Reviews*, vol. 15, no. 8, pp. 3963-3979, Oct. 2011, doi: 10.1016/J.RSER.2011.07.024.
- [8] B.-S. Park, M. Usman, M. Imran, and A. Pesyridis, "Review of Organic Rankine Cycle experimental data trends," *Energy Convers Manag*, vol. 173, pp. 679-691, Oct. 2018, doi: 10.1016/J.ENCONMAN.2018.07.097.
- [9] B. Ebrahimpour, P. Hajjaligol, M. Boroushaki, and M. Behshad, "Modeling and techno - economic study of a solar reverse osmosis desalination plant," *International Journal of Environmental Science and Technology*, no. 0123456789, 2022, doi: 10.1007/s13762-022-04099-7.
- [10] L. O. Agbereghe *et al.*, "Investigation of a Hybridized Cascade Trigeration Cycle Combined with a District Heating and Air Conditioning System Using Vapour Absorption Refrigeration Cooling: Energy and Exergy Assessments," *Energies (Basel)*, vol. 17, no. 6, Mar. 2024, doi: 10.3390/en17061295.
- [11] M. Ennio and M. Astolfi, *Organic Rankine Cycle (ORC) Power Systems: Technologies and Applications*. 2016.
- [12] O. İ. M. M. Mohammedsalih and B. G. B. Kılıç, "Experimental investigation of low - temperature organic Rankine cycle using waste heat from gas turbine bearings for different conditions," pp. 1519-1530, 2022, doi: 10.1007/s13762-021-03172-x.
- [13] Y. Le Nian and W. L. Cheng, "Insights into geothermal utilization of abandoned oil and gas wells," *Renewable and Sustainable Energy Reviews*, vol. 87, no. November 2017, pp. 44-60, 2018, doi: 10.1016/j.rser.2018.02.004.

- [14] Y. Yang, Y. Huo, W. Xia, X. Wang, P. Zhao, and Y. Dai, "Construction and preliminary test of a geothermal ORC system using geothermal resource from abandoned oil wells in the Huabei oil field of China," *Energy*, vol. 140, pp. 633-645, 2017, doi: 10.1016/j.energy.2017.09.013.
- [15] K. Wang, B. Yuan, G. Ji, and X. Wu, "A comprehensive review of geothermal energy extraction and utilization in oilfields," Sep. 01, 2018, *Elsevier B.V.* doi: 10.1016/j.petrol.2018.05.012.
- [16] J. Patihk, D. Warner-Lall, D. Alexander, R. Maharaj, and D. Boodlal, "The optimization of a potential geothermal reservoir using abandoned wells: a case study for the forest reserve field in Trinidad," *J Pet Explor Prod Technol*, vol. 12, no. 1, pp. 239-255, 2022, doi: 10.1007/s13202-021-01322-y.
- [17] S. Gharibi, E. Mortezaazadeh, S. Jalaledin, H. Aghchegh, and A. Vatani, "Feasibility study of geothermal heat extraction from abandoned oil wells using a U-tube heat exchanger," *Energy*, vol. 153, pp. 554-567, 2018, doi: 10.1016/j.energy.2018.04.003.
- [18] G. Li, "Organic Rankine cycle environmental impact investigation under various working fluids and heat domains concerning refrigerant leakage rates," *International Journal of Environmental Science and Technology*, vol. 16, no. 1, pp. 431-450, 2019, doi: 10.1007/s13762-018-1686-y.
- [19] A. Midilli and I. Dincer, "Development of some exergetic parameters for PEM fuel cells for measuring environmental impact and sustainability," *Int J Hydrogen Energy*, vol. 34, no. 9, pp. 3858-3872, 2009, doi: 10.1016/j.ijhydene.2009.02.066.
- [20] I. Dincer and M. A. Rosen, *Exergy*. Elsevier Ltd, 2013.
- [21] J. Oyekale and E. Emagbetere, "Impacts of biomass hybridization on exergetic sustainability of a solar organic Rankine cycle power plant," *Proceedings of the Institution of Mechanical Engineers, Part E: Journal of Process Mechanical Engineering*, 2022, doi: 10.1177/09544089221099881.
- [22] L. Meyer, G. Tsatsaronis, J. Buchgeister, and L. Schebek, "Exergoenvironmental analysis for evaluation of the environmental impact of energy conversion systems," *Energy*, vol. 34, no. 1, pp. 75-89, 2009, doi: 10.1016/j.energy.2008.07.018.
- [23] G. Tsatsaronis and T. Morosuk, "A general exergy-based method for combining a cost analysis with an environmental impact analysis. Part II - Application to a cogeneration system," in *ASME International Mechanical Engineering Congress and Exposition, Proceedings*, 2009, pp. 463-469. doi: 10.1115/IMECE2008-67219.
- [24] K. Parham, H. Alimoradiyan, and M. Assadi, "Energy, exergy and environmental analysis of a novel combined system producing power, water and hydrogen," *Energy*, vol. 134, pp. 882-892, Sep. 2017, doi: 10.1016/j.energy.2017.06.016.
- [25] F. I. Abam, E. B. Ekwe, S. O. Effiom, M. C. Ndukwu, T. A. Briggs, and C. H. Kadurumba, "Optimum exergetic performance parameters and thermo-sustainability indicators of low-temperature modified organic Rankine cycles (ORCs)," *Sustainable Energy Technologies and Assessments*, vol. 30, no. October 2017, pp. 91-104, 2018, doi: 10.1016/j.seta.2018.09.001.

- [26] F. I. Abam, E. B. Ekwe, S. O. Effiom, and M. C. Ndukwu, "A comparative performance analysis and thermo-sustainability indicators of modified low-heat organic Rankine cycles (ORCs): An exergy-based procedure," *Energy Reports*, vol. 4, pp. 110-118, 2018, doi: 10.1016/j.egy.2017.08.003.
- [27] F. I. Abam, E. B. Ekwe, S. O. Effiom, and C. B. Afangideh, "Performance and thermo-sustainability analysis of non-hybrid organic Rankine cycles (ORCs) at varying heat source and evaporator conditions," *Australian Journal of Mechanical Engineering*, vol. 16, no. 3, pp. 238-248, Sep. 2018, doi: 10.1080/14484846.2017.1373585.
- [28] V. Adebayo, M. Abid, M. Adedeji, and T. A. Hussain Ratlamwala, "Energy, exergy and exergo-environmental impact assessment of a solid oxide fuel cell coupled with absorption chiller & cascaded closed loop ORC for multi-generation," *Int J Hydrogen Energy*, vol. 47, no. 5, pp. 3248-3265, 2022, doi: 10.1016/j.ijhydene.2021.02.222.
- [29] N. Nasruddin, I. Dwi Saputra, T. Mentari, A. Bardow, O. Marcelina, and S. Berlin, "Exergy, exergoeconomic, and exergoenvironmental optimization of the geothermal binary cycle power plant at Ampallas, West Sulawesi, Indonesia," *Thermal Science and Engineering Progress*, vol. 19, no. November 2019, p. 100625, 2020, doi: 10.1016/j.tsep.2020.100625.
- [30] M. Alibaba, R. Pourdarbani, M. H. Khoshgoftar Manesh, I. Herrera-Miranda, I. Gallardo-Bernal, and J. L. Hernández-Hernández, "Conventional and advanced exergy-based analysis of hybrid geothermal-solar power plant based on ORC cycle," *Applied Sciences (Switzerland)*, vol. 10, no. 15, 2020, doi: 10.3390/app10155206.
- [31] Y. Ding, C. Liu, C. Zhang, X. Xu, Q. Li, and L. Mao, "Exergoenvironmental model of Organic Rankine Cycle system including the manufacture and leakage of working fluid," *Energy*, vol. 145, pp. 52-64, 2018, doi: 10.1016/j.energy.2017.12.123.
- [32] Z. Fergani, D. Touil, and T. Morosuk, "Multi-criteria exergy based optimization of an Organic Rankine Cycle for waste heat recovery in the cement industry," *Energy Convers Manag*, vol. 112, pp. 81-90, 2016, doi: 10.1016/j.enconman.2015.12.083.
- [33] X. Hu, J. Banks, L. Wu, and W. Victor, "Numerical modeling of a coaxial borehole heat exchanger to exploit geothermal energy from abandoned petroleum wells in Hinton, Alberta," *Renew Energy*, vol. 148, pp. 1110-1123, 2020, doi: 10.1016/j.renene.2019.09.141.
- [34] P. Idialu, J. Ainodion, and L. Alabi, "Restoration and Remediation of Abandoned Petroleum Drill Sites - A Nigerian Case Study," Mar. 29, 2004. doi: 10.2118/86796-MS.
- [35] J. J. García-Pabón, D. Méndez-Méndez, J. M. Belman-Flores, J. M. Barroso-Maldonado, and A. Khosravi, "A review of recent research on the use of r1234yf as an environmentally friendly fluid in the organic rankine cycle," *Sustainability (Switzerland)*, vol. 13, no. 11, 2021, doi: 10.3390/su13115864.
- [36] A. Lazzaretto and G. Manente, "A new criterion to optimize ORC design performance using efficiency correlations for axial and radial turbines," *International Journal of Thermodynamics*, vol. 17, no. 3, pp. 173-181, 2014, doi: 10.5541/ijot.562.

- [37] A. Borsukiewicz-gozdur and W. Nowak, "Geothermal Power Station with Supercritical Organic Cycle Principles of operations of a power," *World Geothermal Congress*, no. April, pp. 25-29, 2010.
- [38] H. Aydin, "Exergetic sustainability analysis of LM6000 gas turbine power plant with steam cycle," *Energy*, vol. 57, pp. 766-774, 2013, doi: 10.1016/j.energy.2013.05.018.
- [39] "Environmental Management - Life Cycle Assessment - Requirements and Guidelines, I. 14044 International Organization for Standardization (ISO)," 2006.
- [40] M. Goedkoop and R. Spriensma, "The Eco-indicator 99 - A damage oriented method for Life Cycle Impact Assessment," 2001.
- [41] "ecoinvent v3.7.1 - ecoinvent." Accessed: Jan. 11, 2022. [Online]. Available: <https://ecoinvent.org/the-ecoinvent-database/data-releases/ecoinvent-3-7-1/>
- [42] G. Wernet, C. Bauer, B. Steubing, J. Reinhard, E. Moreno-Ruiz, and B. Weidema, "The ecoinvent database version 3 (part I): overview and methodology," *International Journal of Life Cycle Assessment*, vol. 21, no. 9, pp. 1218-1230, 2016, doi: 10.1007/s11367-016-1087-8.
- [43] J. Oyekale, M. Petrollese, D. Cocco, and G. Cau, "Energy Conversion and Management: X Annualized exergoenvironmental comparison of solar-only and hybrid solar-biomass heat interactions with an organic Rankine cycle power plant," *Energy Conversion and Management: X*, vol. 15, no. April, p. 100229, 2022, doi: 10.1016/j.ecmx.2022.100229.
- [44] A. Lazzaretto and G. Tsatsaronis, "SPEC0: A systematic and general methodology for calculating efficiencies and costs in thermal systems," *Energy*, vol. 31, no. 8-9, pp. 1257-1289, 2006, doi: 10.1016/j.energy.2005.03.011.
- [45] E. Y. Gürbüz, O. V. Güler, and A. Keçebaş, "Environmental impact assessment of a real geothermal driven power plant with two-stage ORC using enhanced exergo-environmental analysis," *Renew Energy*, vol. 185, pp. 1110-1123, 2022, doi: 10.1016/j.renene.2021.12.097.

NOMENCLATURE

Symbols

\dot{RE}_D	relative destroyed exergy (irreversibility)
\dot{m}	mass flow rate (kg/s)
\dot{q}	heat flux (W/m ²)
\dot{W}	electrical power (kW)
\dot{B}	exergo-environmental rate (€/h)
\dot{E}	rate of exergy (kW)
\dot{i}	rate of destroyed exergy (kW)
\dot{Q}	thermal power (kW)

b	specific exergo-environmental impact (Pt/kWh)
e	specific exergy (kJ/kg)
f_b	exergo-environmental factor
h	enthalpy (kJ/kg)
int	interest rate
MF	maintenance factor
N	plant lifetime (years)
s	entropy (kJ/kgK)
SUB ORC	subcritical ORC without a recuperator
SUB-REGEN ORC	subcritical ORC with a recuperator
T	temperature (°C)
Y	environmental impact point (Pt)

Greek letters

ε	exergetic (rational) efficiency
δ	efficiency defect

Subscripts

i	inlet side
o	outlet side

Abbreviations

ORC	organic Rankine cycle
-----	-----------------------

APPENDIX

Definitions of exergo-environmental metrics employed in the study for a generic component k:

$$b_{f,k} = \frac{B_{f,k}}{E_{f,k}}$$

$$b_{p,k} = \frac{B_{p,k}}{E_{p,k}}$$

$$B_{D,k} = b_{f,k} \times I_k$$



$$BRT_k = B_{D,k} + Y_k$$

$$f_{b,k} = \frac{Y_k}{B_{I,k} + Y_k}$$

$$r_{b,k} = \frac{b_{p,k} - b_{f,k}}{b_{f,k}}$$

$$EIE_k = \frac{BRT_k}{\dot{W}_{net}}$$

DETERMINATION OF RADON GAS LEVELS IN THE AIR IN THE FACULTY BUILDING (BİTLİS)

Sultan Şahin Bal ^{1, *} , Yonca Dervişoğlu Koç ² 

¹ Bitlis Eren University, Department of Physics, Türkiye, ssahin@beu.edu.tr

² Bitlis Eren University, Department of Physics, Türkiye, dervisogluyonca@gmail.com

* Corresponding author

KEYWORDS

Radon
AEDE
ELCR
AlphaGuard
Faculty
Bitlis

ARTICLE INFO

Research Article

DOI:

[10.17678/beuscitech.1485248](https://doi.org/10.17678/beuscitech.1485248)

Received 19 May 2024

Accepted 8 August 2024

Year 2024

Volume 14

Issue 2

Pages 103-118



ABSTRACT

Living things are exposed to internal and external natural radiation throughout their lives. Natural radiation consists mostly of cosmic rays and terrestrial radiation sources containing many radioisotopes. While uranium, thorium and potassium are the main radionuclides that constitute terrestrial natural radiation sources; radon is a radioactive gas that occurs naturally by the decay of uranium found in soil, rocks and water. People are mostly exposed to natural radiation due to building construction materials and indoor radon concentration.

In this study, measurement of radon gas activity concentration levels in the air in Bitlis Eren University Faculty of Science and Letters building was made using an active radon measurement detector (AlphaGUARD). As a result of these measurements; The average radon activity concentration was determined as 41.13 Bq/m³. When the measurement results are compared with the limit values; It has been determined that there is no risk to health. Annual effective dose equivalent, AEDE, (average 0.889 mSv/y) and excess lifetime cancer risk, ELCR, (average 3.545) parameters were calculated using radon activity concentration values.

1 INTRODUCTION

Radioactive isotopes that have been present in the structure of the earth's crust since the formation of the earth and high-energy cosmic rays coming from space are the sources of natural radiation. Natural radioactive isotopes found in many environments such as soil, water, air, vegetation, foods and building materials cause external and internal irradiation of our body [1].

The first of the main components of the natural radiation in the environment is the radiation resulting from the decay of uranium, thorium series radionuclides and ^{40}K , which have existed since the formation of the world. The second is cosmic radiation [2].

Living things on earth are exposed to radiation every day from natural radiation sources in the air, water, soil, and even within their own bodies, as well as artificial radiation sources produced by humans. While exposure from natural radiation sources is 80%, exposure from man-made radiation sources is 20% [3].

People spend most of their time in indoor environments. In this regard, the quality of the inhaled air is very important for human health. Along with beneficial gases such as nitrogen, oxygen and hydrogen, harmful gases are also present in the environment. Radon gas, formed as a result of the decay of uranium, is among the gases harmful to human health. Since 1960, as the knowledge that radon gas is concentrated in buildings and causes lung cancer has become widespread, research on determining radon concentration levels in indoor environments has gained importance and maps have been prepared to determine radon activity concentration levels. The Turkish Atomic Energy Agency (TAEK, today known as the Turkish Energy, Nuclear and Mining Research Council (TENMAK)) started working on this subject in 1984, but the radon map of our country has not been completed yet [4]. In order to create a radon map, environmental radon activity concentration measurements are carried out in our country.

Considering that people spend most of their time in closed environments in our country and that a large number of cancer diagnoses are made, the importance of determining indoor ^{222}Rn gas concentrations for human health becomes evident. When the studies carried out in the world and in our country in recent years are

examined, it turns out that the biggest cause of lung cancer, especially after smoking, is ^{222}Rn gas. Based on these studies, 3% to 14% of lung cancer cases are thought to be caused by ^{222}Rn [5].

In this study, radon activity concentration levels in the air were determined in some offices located in the Bitlis Eren University Faculty of Science and Letters building. The results of the measurements and calculations were interpreted, taking into account the limits set by the literature and health organizations, and their effects on human health.

2 MATERIAL AND METHODS

2.1 Geological Formation of Bitlis

Bitlis province is located in the Upper Murat-Van Section of the Eastern Anatolia Region. It is surrounded by the provinces of Ağrı and Muş in the north, Van in the east, Batman in the west, and Siirt in the south. Bitlis province consists of 7 districts: the central district, Tatvan, Ahlat, Güroymak, Adilcevaz, Hizan and Mutki [6].

There are various stratigraphic sections throughout the Bitlis Metamorphic belt. No classification study has been carried out according to the acidity and alkalinity values of the rocks of Bitlis province.

Bitlis' rock sequence; Pre-Devonian Lower Unit, Devonian-Upper Triassic Upper Unit, Guleman Group including meta-ophiolites, Kinzu Formation consisting of flysch type sediments and Paleocene-Lower Eocene aged Maden Group sediments are distinguished [7].

In some places within the Upper Unit in the Bitlis rock sequence, there are Mesozoic-Tertiary aged greenstone blocks at faulted contacts with phyllite and pelitic schists. Lateral discontinuity and blocky appearance of durable units such as limestone and quartzite in this unity are observed in many places. The existence of two units, whose relations are regulated by tectonic events, has been shown in the complex structured mass called Bitlis massif [8].

2.2 Geological Formation of Rahova

Rahva plain is located in the Upper Euphrates Section of the Eastern Anatolia Region. This plain, which is within the borders of Bitlis province; It has the feature of a water division line separating the Euphrates, Tigris and Van Lake basins from each other. In other words, Rahva is a threshold area that determines the common boundaries of three hydrographic basins.

In the parts of the Rahva plain close to the Bitlis Mountains, the valleys are buried deeper. The rocks cropping out along the valleys consist of trachyandesitic tuffs and ignimbrites. The volcanics that make up the plain are listed as brownish-red tuff (also called poorly welded ignimbrite) at the top, gray-brown ash below, and light-colored, well-welded trachyandesitic ignimbrite at the bottom, respectively.

Rahva plain is a threshold area between the metamorphic Bitlis old mass and the Nemrut volcano formed as a result of Plio-Quaternary volcanism. While the basic formations of this area consist of schists and recrystallized limestones, the sections close to the surface consist entirely of volcanic formations [9].

2.3 Determination of Radon in Air with AlphaGuard

AlphaGUARD PQ 2000PRO, used in Radon measurements, is a portable radiation detector used to measure the radiation intensities and Gamma (γ) dose rate of Radon (Radon-222), Radon-220 (Thoron) and Radon by-products. AlphaGUARD can make radiation measurements in air, water, soil and building materials. Measurement results; AlphaGUARD detector, which gives Bq (Becquerel) per volume, that is, Bq/m³, can simultaneously measure three different climatic parameters such as temperature, atmospheric pressure and humidity [10].

The AlphaGUARD Radon detector draws air into the detector ionization chamber with the help of a suction pump integrated into the measurement unit. ²²²Rn and ²²⁰Rn isotopes entering the ionization chamber as a result of absorption decay and create electrical signals by causing ionization in the chamber. During this continuous absorption, Radon byproducts are retained by a plate-shaped filter, and the alpha activity of Radon daughter products accumulated on the filter plate is measured by the alpha-sensitive TN-WL-02 microchip module, which is a sensitive digital processor module placed on the other side of the filter plate. The electrical

signals obtained from all measurements are sent as a TTL signal to the Counter-Module counter unit of the AlphaGUARD PQ 2000PRO and are converted into readable data by the software using the calibration information of the detector [10].

The software package (DataEXPERT) developed for AlphaGUARD was used to graphically process, develop, archive and present the received data in a virtual environment.

There is no need for additional equipment with the detector to measure radon concentration in air. On the AlphaGUARD device, '10 min DIFFUSION' was selected as the measurement mode. The detector was positioned approximately 1.5-2 m above the ground in the working environment. The AlphaGUARD radon detector draws air into the detector ionization chamber with the help of a suction pump integrated into the measurement unit. Measurements were made for 24 hours for each study area in order to observe the transitions between day and night and the effect of ventilation on the radon concentration in the environment. In order to make scientific interpretations of the data stored during the measurement, AlphaGUARD was connected to the computer and worked with data analysis software (DataEXPERT) [10].

2.4 Annual effective dose equivalent (AEDE)

Quantification of the effects of ionizing radiation to which humans are exposed from air, water and food sources is carried out by calculating the physical quantity called the annual effective dose. The dose exposed over a period of 1 year is defined as the annual effective dose. Annual effective dose equivalent calculation was made using the following Equation 1 [11], [12];

$$AEDE(Sv/y) = A_{Rn} \times DP \times EECC \times T \quad (1)$$

AEDE; annual effective dose equivalent (mSv/y), DP; balance factor between radon and its decay products (0.4), EECC; equilibrium equivalent concentration coefficient (9×10^{-9} (Sv/hour)/(Bq/m³)), T; total working day hours in 2020 (6,000 hours/year).

2.5 Excess lifetime cancer risk (ELCR)

ELCR is a reasonable upper bound estimate of a person's probability of developing cancer sometime in their life after any radiation exposure [13], [14]. Excess lifetime cancer risk calculation was made using the following Equation 2 [11], [12];

$$ELCR = AEDE \times LE \times FRF \quad (2)$$

LE; life expectancy of people (70 years), FRF; fatal risk factor stated in the ICRP report (0.057 Sv⁻¹) [15].

3 RESULTS

In this study; ²²²Rn concentration in the air, temperature, pressure and relative humidity measurements were made in the Bitlis Eren University Faculty of Science and Letters building. The radon measurement results obtained using the AlphaGUARD active radon measurement device were analysed using the DataEXPERT software for spectrum analysis. Sample graphs of the measurements made are shown in Figure 1.



Figure 1. Sample graphs of measurements taken from the faculty building (a: ^{222}Rn activity concentration, b: temperature, c: pressure, d: relative humidity).

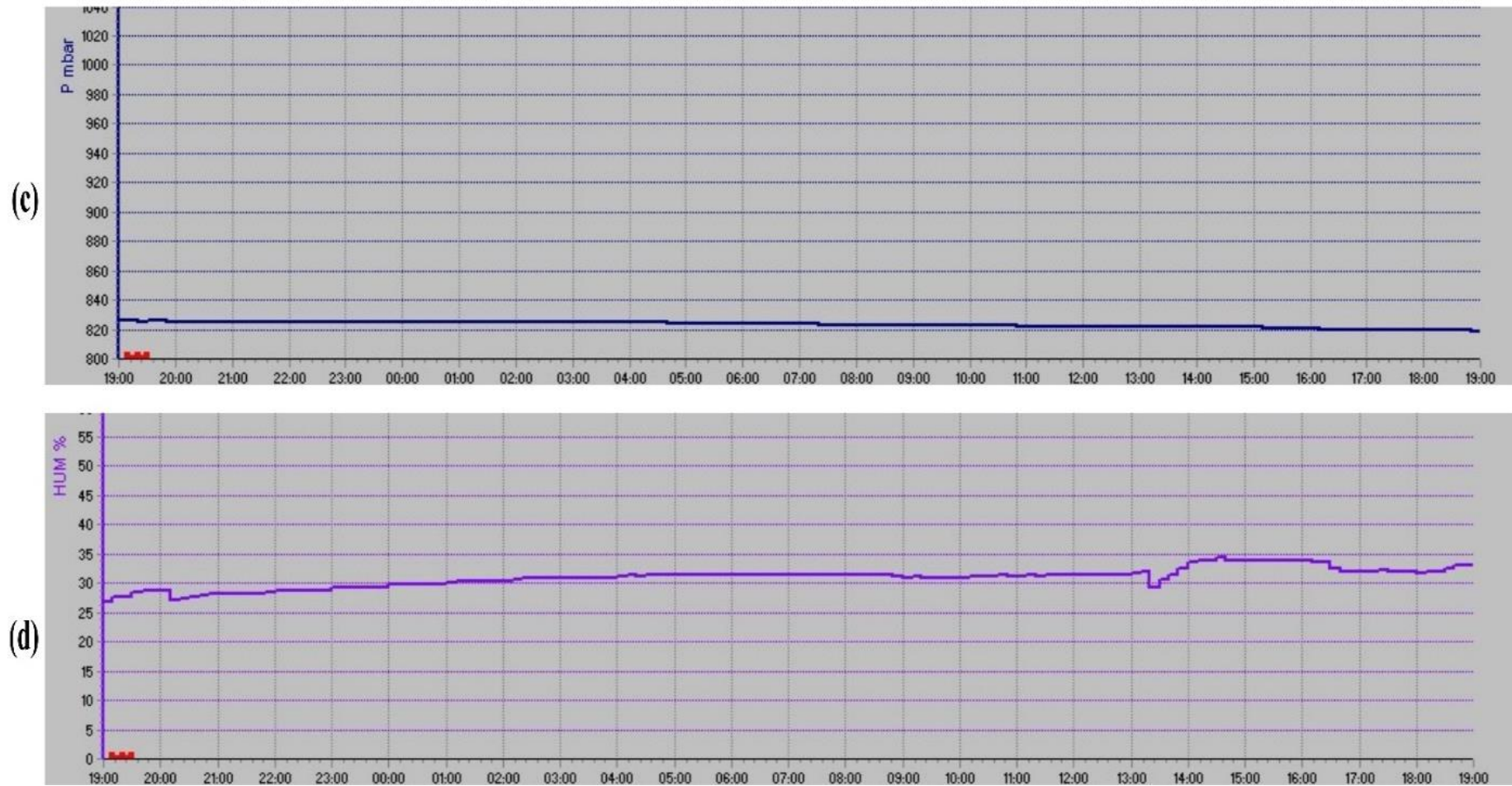


Figure 2. (Continuous) Sample graphs of measurements taken from the faculty building (a: ^{222}Rn activity concentration, b: temperature, c: pressure, d: relative humidity).

Table 1. Radon activity concentration in the air and some atmospheric data of the measured rooms in the Faculty of Science and Letters building.

Measure No		Starting date/time	End date/time	²²² Radon (Bq/m ³)	Temperature (°C)	Pressure (mbar)	Humidity (% rH)	AEDE (mSv/y)	ELCR x 10 ⁻³
1	Ground Room 1	18.11.2020/ 16.00	19.11.2020/ 16.00	34 ± 12	24.2	814	29.0	0.734	2.930
2	Ground Room 2	19.11.2020/ 16.05	20.11.2020/ 16.05	30 ± 11	24.6	818	28.3	0.648	2.586
3	Ground Room 3	20.11.2020/ 16.07	21.11.2020/ 16.07	31 ± 11	24.0	810	28.2	0.670	2.672
4	Floor 1 Room 1	16.11.2020/ 15.50	17.11.2020/ 15.50	29 ± 11	25.8	815	31.8	0.626	2.499
5	Floor 1 Room 2	17.11.2020/ 15.55	18.11.2020/ 15.55	8 ± 5	24.8	824	26.4	0.173	0.690
6	Floor 1 Room 3	23.11.2020/ 13.30	24.11.2020/ 13.30	30 ± 11	24.7	823	30.9	0.648	2.586
7	Floor 2 Room 1	24.11.2020/ 13.35	25.11.2020/ 13.35	23 ± 9	24.8	826	20.0	0.497	1.982
8	Floor 2 Room 2	26.11.2020/ 13.50	27.11.2020/ 13.50	47 ± 12	27.2	819	20.9	1.015	4.051
9	Floor 2 Room 3	27.11.2020/ 13.55	28.11.2020/ 13.55	25 ± 10	26.8	825	22.7	0.540	2.155
10	Floor 3 Room 1	30.11.2020/ 13.10	01.12.2020/ 13.10	51 ± 15	25.2	821	25.6	1.102	4.395
11	Floor 3 Room 2	07.12.2020/ 14.20	08.12.2020/ 14.20	25 ± 10	22.7	821	30.3	0.540	2.155
12	Floor 3 Room 3	08.12.2020/ 14.25	09.12.2020/ 14.25	33 ± 13	23.9	821	29.0	0.713	2.844
13	Floor 4 Room 1	09.12.2020/ 14.30	10.12.2020/ 14.30	43 ± 11	23.7	822	28.4	0.929	3.706
14	Floor 4 Room 2	15.12.2020/ 13.30	16.12.2020/ 13.30	106 ± 14	24.5	817	29.9	2.290	9.136
15	Floor 4 Room 3	16.12.2020/ 13.50	17.12.2020/ 13.50	102 ± 16	22.5	819	35.3	2.203	8.791
	Average			41.13 ± 11	24.6	819.7	27.8	0.889	3.545

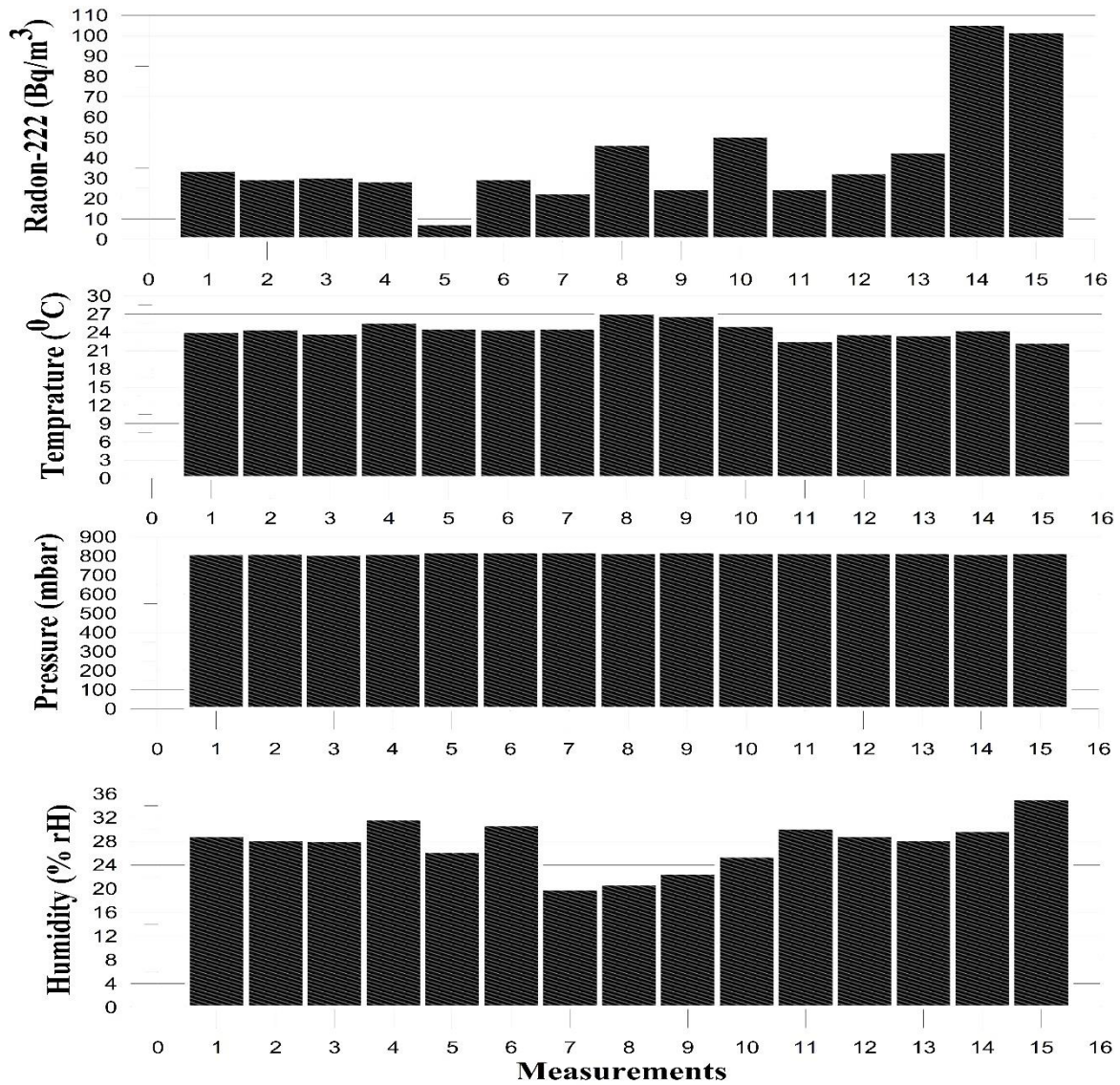


Figure 2. Display of radon activity concentration and some atmospheric data.

When Table 1 and Figure 2 are examined; ²²²Rn activity concentration between 8 (1st floor) and 106 (4th floor) Bq/m³, temperature values between 22.5 and 27.2 °C, pressure values between 810 and 826 mbar, relative humidity values between 20.0 and 35.3 %rH appears to have changed.

The rooms where measurements are made are generally working offices where air circulation is available. Since the offices are closed in the evenings, average values of 24-hours measurements were read from the measuring device.

When examining the variation of radon measurement values according to floors, it was generally observed that the radon activity concentration values

measured on the same floors were approximately similar. The 4th (measure in the Floor 1/Room 1) and 5th (measure in the Floor 1/Room 1) radon activity concentration measurements were taken from different study rooms on the same floor. However, it was noted that there was a significant difference between these two measurements. The reason for the 5th measurement being much lower than the 4th could be due to extensive ventilation in the room. Upon detailed examination of the rooms in terms of physical and many other factors, it was found that there were no factors (other than ventilation) that could account for this difference.

The radon activity concentration values of measurements 14 and 15 are observed to be significantly higher than those of the other measurements. These measurements were taken in the offices located on the fourth floor of the building. Similar studies in the literature have shown that indoor radon activity concentration values decrease as you move from the ground floor to the upper floors [16], [17]. This study was conducted during the pandemic period (2020-2021). During this time, schools were closed, and/or remote education was being conducted. As a result, many offices remained closed for weeks and were not ventilated. The offices where measurements 14 and 15 were taken were among these and were not ventilated for a long period. During the winter months, the indoor air being warmer than the outdoor air can create low pressure inside the building, increasing the radon activity concentration [16], [17]. The lack of ventilation for an extended period during that time may have caused these measurements to be significantly higher than the others.

Radon activity concentration varies regionally because the main source of radon is uranium. Because; Limit values of radon activity concentration also vary between countries. The limit value is accepted as 200 Bq/m³ in the UK, 400 Bq/m³ in European countries, and 800 Bq/m³ in Canada. Within the framework of the International Atomic Energy Agency Essential Safety Standards (IAEA-BSS), recommended levels for radon in homes are determined as 200-600 Bq/m³. According to the Atomic Energy Authority Radiation Safety Regulation in Turkey, the allowed limit value for homes is 400 Bq/m³ and for workplaces it is 1000 Bq/m³ [18].

Table 2. Radon activity concentration values of some similar studies.

Location	Average Radon-222 (Bq/m ³)	References
Isparta (faculty buildings)	220	[19]
İstanbul (school buildings)	125.06	[20]
Nevşehir (school buildings)	67	[21]
İstanbul (faculty buildings)	24.6	[22]
İstanbul (faculty buildings)	14.47	[23]
Kastamonu (school buildings)	28.43	[10]
Kırklareli (faculty buildings)	16.78	[17]
This study	41.13	

According to the standards set by Turkish Energy, Nuclear and Mineral Research Agency (TENMAK) and various organizations in other countries and the results of similar studies conducted in our country (Table 2), it is seen that the results obtained in this study (average radon activity concentration 41.13 Bq/m³) are below the permissible limits and the results of similar studies.

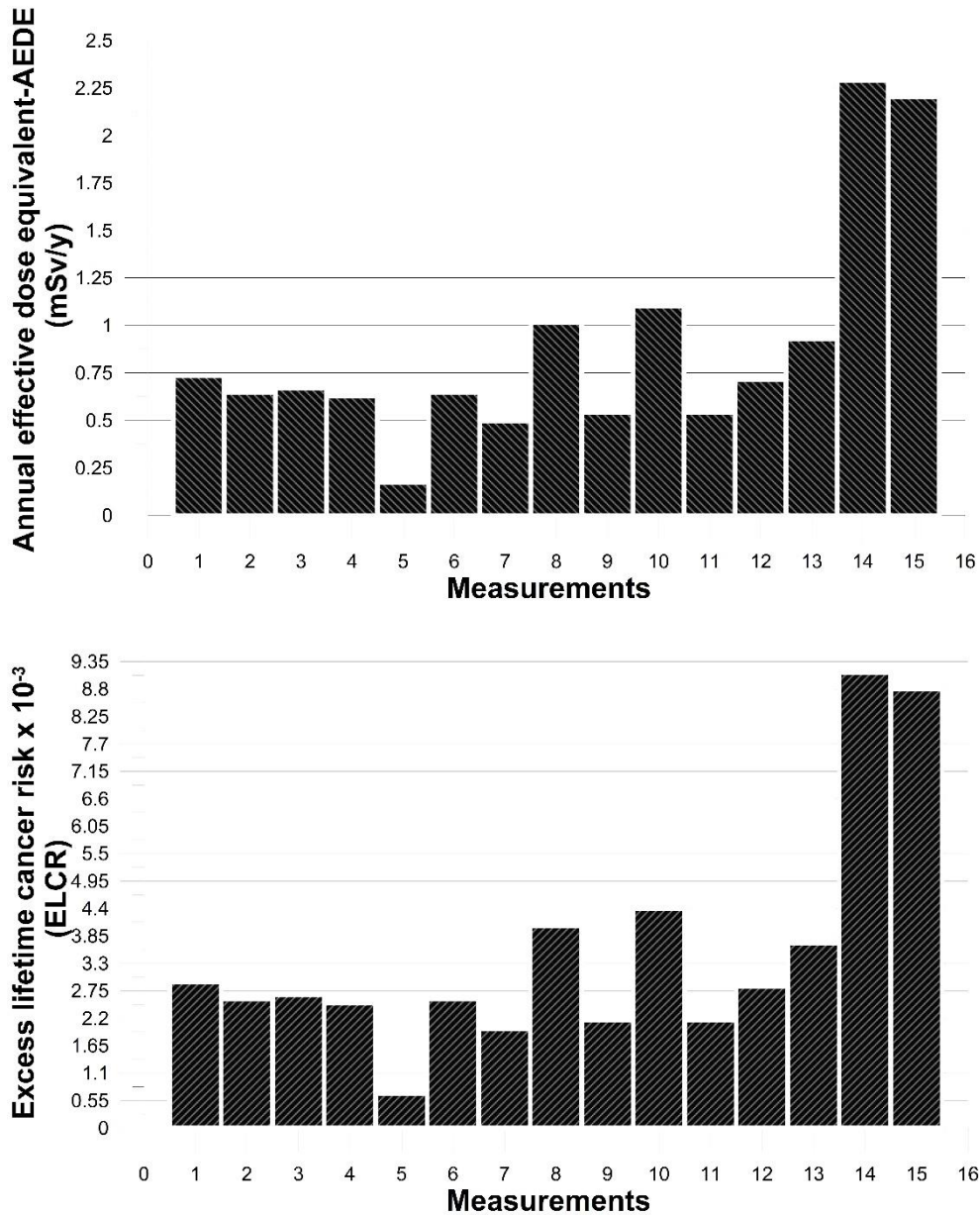


Figure 3. Display of annual effective dose equivalent and excess lifetime cancer risk.

When Table 1 and Figure 3 are examined; annual effective dose equivalent (AEDE) between 0.173 (1st floor) and 2.290 (4th floor) mSv/y, excess lifetime cancer risk (ELCR) values between 0.692 and 9.136 appears to have changed.

According to TENMAK, the external irradiation dose originating from the earth (inside the building) is 0.41 mSv/y, depending on the mixture of soil and building materials. In addition to this value, the respiratory irradiation dose depending on the radon gas concentration is 1.15 mSv/y. Depending on both factors in the office rooms

where measurements are taken, the total dose (limit value) is calculated as 1.56 mSv/y.

It is seen that AEDE values in offices 2 (2.290 mSv/y) and 3 (2.203 mSv/y) on the 4th floor of the faculty building are above the 1.56 mSv/y limit value. The average value of AEDE was calculated as 0.889 mSv/y. The average value is below the limit value and the calculated values are generally found to be risk-free. When ELCR values are examined, it is seen that the overall risk of cancer is not high.

4 CONCLUSION

It was determined that the radon-222 activity concentration level (average 41.13 Bq/m³) measured in the Bitlis Eren University Faculty of Science and Letters building was below the limit values determined both in our country and in other countries. Since the measured radon activity concentration values are below the limit values, it shows that there is no risk to health. Radon activity concentration values were determined by measuring on various floors of the faculty building. According to the measured results, it was determined that the radon activity concentration value did not change depending on the floors. According to this study, it was observed that radon activity concentration values were not affected much by atmospheric parameters such as temperature, pressure and relative humidity.

It was observed that AEDE values were not alarming considering the limit value (1.56 mSv/y). However, it can be said that ELCR values do not pose a risk.

Ventilating offices periodically will reduce the radon gas that naturally accumulates in the office, and in this way, an important precaution will be taken in terms of health.

Conflict of interest

There is no conflict of interest between the authors.

Authors Contributions

Writing the article, processing and reviewing the data, and calculations were made by Sultan ŞAHİN BAL. Radon measurements were made by Yonca DERViŞOĞLU KOÇ.

Statement of Research and Publication Ethics

The study is complied with research and publication ethics.

REFERENCES

- [1] A. Kurt, "Determination of Indoor Air Radon Concentrations in Primary Schools in Fatih District of Istanbul Province," M.S. thesis, Science. Inst., İstanbul Univ., İstanbul, Türkiye, 2015.
- [2] E. Fidan, "Adapazarı central winter radon measurement and analysis," M.S. thesis, Science. Inst., İstanbul Technic Univ., İstanbul, Türkiye, 2009.
- [3] A. Kaderoğlu, N. Kaya, V. E. Karaaslan and Y. S. Koç, "Ministry of National Education 12th Grade Physics Textbook". Accessed: June, 08, 2023. [Online]. Available: <https://ogmmateryal.eba.gov.tr/panel/upload/etkilesimli/kitap/fenlisesifizik/12/unite4>
- [4] F. Cabi Değerli and F. Umaroğulları, "Radon in Buildings and Its Effects on Health". Accessed: February, 04, 2023. [Online]. Available: https://www.yesilbinadergisi.com/yayin/264/binalarda-radon-ve-saglik-uzerindeki-etkileri_7919.html#.Y92G33ZBzIU
- [5] WHO, Handbook on Indoor Radon: A Public Health Perspective. World Health Organization, Geneva, Switzerland, 2009.
- [6] N. Elmastaş, "Geothermal spring in Bitlis province," Eastern Geographical Review, vol.13, no. 19, pp. 89-104, 2011.
- [7] M. C. Göncüoğlu and N. Turhan, "New age findings in Bitlis metamorphites," Journal of Mineral Research and Exploration, vol. 95-96, pp. 1-5, 1981.
- [8] A. Boray, "The Structure and Metamorphism of the Bitlis Area," Türkiye Geoi. Founding Bulletin, vol. 95-96, pp. 1-5, 1981.
- [9] K. Arınç, "An analysis of the vicinity of the smoothness of Rahva with regard to transportation geography," Eastern Geography Journal, vol. 6, no. 3, pp. 25-46, 2000.
- [10] G. Aras, "Measurement of Airborne Radon Activity in School Buildings in Kastamonu Center," M.S. thesis, Science. Inst., Kastamonu Univ., Kastamonu, Türkiye, 2011.
- [11] K. Karatay, "Determination of indoor radon concentration in Yahya Kaptan District of Kocaeli province," M.S. thesis, Science. Inst., Kocaeli Univ., Kocaeli, Türkiye, 2016.
- [12] S. Şahin Bal, "The determination of concentrations of radioisotopes in some granite samples in Turkey and their radiation hazards", Radiation Effects and Defects in Solid, vol. 173, pp. 353-366, 2018, doi: 10.1080/10420150.2018.1462358.

- [13] S. C. Freni, "Appiction of estimated excess lifetime cancer risk in field situations", *Uncertainty in Risk Assessment, Risk Management and Decision Making*, Vol. 4, pp. 339-347, 1987, https://doi.org/10.1007/978-1-4684-5317-1_27
- [14] J.V. McDonald, "Hopewell precision area contamination-Appendix C- NYS DOH procedure for evaluating potential health risks for contaminants of concern". Accessed: May, 08, 2024. [Online]. Available: <https://www.health.ny.gov/environmental/investigations/hopewell/appendc.htm#:~:text=An%20estimated%20increased%20excess%20lifetime,following%20exposure%20to%20that%20contaminant>
- [15] ICRP, *The 2007 Recommendations of the International Commission on Radiological Protection*, ICRP, ICRP Publication 103. Ann. ICRP 37 (2-4), 2007.
- [16] H. Soğukpınar, "Determination of Seasonal Correction Factors for Indoor Radon Concentrations in Eskişehir Province," PhD thesis, Science. Inst., Eskişehir Osman Gazi Univ., Eskişehir, Türkiye, 2013.
- [17] M. Tamir Darcan, "Indoor radon gas measurement at Kırklareli University Kayalı Campus," M.S. thesis, Science. Inst., Kırklareli Univ., Kırklareli, Türkiye, 2020.
- [18] TENMAK, "Natural radiation sources". Accessed: March, 08, 2024. [Online]. Available: <https://www.tenmak.gov.tr/2016-06-09-00-43-46/1087-dogal-radyasyon-kaynaklari.html>
- [19] M.E. Kürçüoğlu and G. Bayraktar, "Determination of indoor radon concentrations at Süleyman Demirel University using nuclear trace detectors", *Journal of Süleyman Demirel Univ. Inst. Sci. Tech.*, Vol. 16, no. 2, pp. 167-183, 2012.
- [20] A. Kurt, "Determination of indoor air radon concentrations in primary schools in Fatih district of İstanbul province," M.S. thesis, Science. Inst., İstanbul Univ., İstanbul, Türkiye, 2015.
- [21] S. Akyürek, "Measurement of radon gas concentration in schools located in Nevşehir city center with active method and evaluation of annual effective radiation dose," M.S. thesis, Science. Inst., Hacı Bektaş Veli Univ., Nevşehir, Türkiye, 2017.
- [22] F. Kulalı, O. Günay and S. Aközcan, "Determination of Indoor Radon Levels at Campuses of Uskudar and Okan Universities", *Int. Journal of Environ. Sci. Tech.*, Vol. 16, pp. 5281-5284, 2019.
- [23] O. Günay, S. Aközcan and F. Kulalı, "Measurement of Indoor Radon Concentration and Annual Effective Dose Estimation for a University Campus in İstanbul", *Arab. J Geosci*, Vol. 12, no. 171, pp. 1-8, 2019.